Acta Pharmaceutica Sinica B 2025;15(1):239−255

Chinese Pharmaceutical Association
Institute of Materia Medica, Chinese Academy of Medical Sciences

Acta Pharmaceutica Sinica B

www.elsevier.com/locate/apsb
www.sciencedirect.com

ORIGINAL ARTICLE

Regulation of histidine metabolism by *Lactobacillus Reuteri* mediates the pathogenesis and treatment of ischemic stroke

Kangrui Hu[a,†], Zhihao Zhou[a,†], Haofeng Li[b,†], Jijun Xiao[c], Yun Shen[a], Ke Ding[a], Tingting Zhang[a], Guangji Wang[a,*], Haiping Hao[a,*], Yan Liang[a,*]

[a]*Key Lab of Drug Metabolism & Pharmacokinetics, State Key Laboratory of Natural Medicines, China Pharmaceutical University, Nanjing 210009, China*
[b]*Ministry of Education Key Laboratory of Protein Science, Beijing Advanced Innovation Center for Structural Biology, Beijing Frontier Research Center for Biological Structure, Tsinghua-Peking Center for Life Sciences, School of Life Sciences, Tsinghua University, Beijing 100084, China*
[c]*School of Materials Science and Engineering, Hebei University of Science and Technology, Shijiazhuang 050023, China*

Received 7 May 2024; received in revised form 9 June 2024; accepted 26 July 2024

KEY WORDS

Ischemic stroke;
Inflammation;
Gut−brain axis;
Panax notoginseng saponins;
Lactobacillus reuteri;
Metabolomics;
Histidine;
Histamine

Abstract Increasing evidence has underscored the significance of post-stroke alterations along gut−brain axis, while its role in pathogenesis and treatment of ischemic stroke (IS) remains largely unexplored. This study aimed to elucidate the therapeutic effects and action targets of *Panax notoginseng saponins* (PNS) on IS and explore a novel pathogenesis and treatment strategy of IS *via* profiling the microbial community and metabolic characteristics along gut−brain axis. Our findings revealed for the first time that the therapeutic effect of PNS on IS was microbiota-dependent. Ischemia/reperfusion (I/R) modeling significantly down-regulated *Lactobacilli* in rats, and PNS markedly recovered *Lactobacilli*, particularly *Lactobacillus reuteri* (*L.Reu*). Metabolomics showed a significant reduction in serum histidine (HIS) in clinical obsolete IS patients and rehabilitation period I/R rats. Meanwhile, the *L.Reu* colonization in I/R rats exhibited significant neuroprotective activity and greatly increased HIS in serum, gut microbiota, and brain. Moreover, exogenous HIS demonstrated indirect neuroprotective effects through metabolizing to histamine. Notably, vagus nerve severance in I/R rats was performed to investigate HIS's neuroprotective mechanism. The results

*Corresponding authors.
E-mail addresses: liangyan0679@163.com (Yan Liang), guangjiwang@hotmail.com (Guangji Wang), hhp_770505@hotmail.com (Haiping Hao).
†These authors made equal contributions to this work.

Peer review under the responsibility of Chinese Pharmaceutical Association and Institute of Materia Medica, Chinese Academy of Medical Sciences.

https://doi.org/10.1016/j.apsb.2024.10.003

innovatively revealed that PNS could promote HIS synthesis in gut by enhancing *L.Reu* proportion, thereby increasing intracerebral HIS through peripheral pathway. Consequently, our data provided novel insights into HIS metabolism mediated by *L.Reu* in the pathogenesis and treatment of IS.

1. Introduction

Ischemic stroke (IS), which accounts for about 70%−80% of strokes, is the second cause of death and the primary cause of disability worldwide[1]. Up to now, first-line arterial IS treatment is still limited to intravenous ateplase and mechanical thrombectomy[2]. However, the reperfusion treatment of IS with ateplase and mechanical thrombectomy is limited to 5%−10% of patients due to their narrow effective window[3]. Even worse, the sequelae of stroke, such as physical behavior disorders, memory decline, language disorders, swallowing difficulties, and emotional irritability, have caused significant social and economic burdens[2]. Given the limited treatment options for IS, identifying candidate drugs for new prevention, treatment, and rehabilitation is an urgent requirement.

The human gut microbiota, consisting of approximately ten times the number of human cells, is a highly complex ecosystem involving various species[4]. In recent years, gut microbiota has been proven to regulate host metabolic activity, as well as regulate gut immunity and biological barriers[5]. Various essential physiological functions, including energy balance, fluid homeostasis, immune responses, and emotions, were proved to be regulated by the communication between the gut and brain[6]. The bidirectional communication between the brain and gut was usually defined as the gut-brain axis. According to recent clinical trial reports, up to 50% of stroke patients would experience gastrointestinal complications such as dysbiosis of the gut microbiota, intestinal leakage, intestinal bleeding, constipation, and even intestinal sepsis, which in turn accelerate stroke progression and worsen prognosis[7]. Post-stroke gut−axis dysfunction is a promising research field for identifying novel stroke mechanisms and prevention and treatment strategies. With the advancement of metagenomics and metabolomics technologies, there are increasing reports on the relationship between gut microbiota and IS. Several preclinical and clinical studies demonstrated significant alterations in microbial diversity after ischemic attack[8−10]. For instance, Karlsson et al.[11] revealed that the genomic composition of IS patients was significantly different from that of healthy individuals, with a significant increase in the number of Ruminococcus *spp.* in IS patients and a significant decrease in the proportion of Eubacillus *spp.* And Bacteroides *spp*. Compared with the low stroke risk controls, patients in the high-risk group were found to have lower levels of *Lachnospiraceae* and *Ruminococcaceae*[12]. Thus, intestinal microbiota dysbiosis may be a result of brain injury and a key influencing factor of immune changes after stroke, which has a significant impact on the prognosis of stroke[10].

Growing evidence over the past decade has demonstrated that the impact of gut microbiota on brain prognosis after stroke may be attributed to the function of gut bacteria in producing small neuroactive compounds[8]. Intestinal bacteria can produce short-chain fatty acids (SCFAs) and neurotransmitters with neuroprotective effects (γ-aminobutyric acid, norepinephrine, dopamine, etc.), among which SCFAs can induce T cells to differentiate into effector cells based on the immune environment, and modulate Sigmar-1 receptor-related pathways thereby regulating brain function[13,14]. Furthermore, the supplementation of SCFA to mice before stroke induction has been reported to improve behavioral recovery, modulate cortical network connectivity, and modify histological indicators of synaptic plasticity[15]. In addition to SCFAs, the most extensively studied host-microbial interactions included tryptophan metabolism, as microbial communities could directly or indirectly control the production of serotonin, canine uric acid, and indole derivatives[16]. For instance, tryptophan metabolic pathways were identified in *Clostridium sporogenes*, which could decarboxylate tryptophan to produce the neurotransmitter tryptamine[7]. Moreover, *Lactobacillus reuteri (L.Reu)* was associated with altered levels of circulating tryptophan metabolites[17]. The gut microbiota also participates in the metabolism of histidine (HIS), a bioactive amino acid in the nervous system and a precursor of histamine (HA)[18]. Previous reports showed that mice lacking HA or HA receptors exhibited cognitive and behavioral impairments[19]. However, the relationship between HIS/HA and IS still remains unclear.

After 2000 years of clinical practice, it was proved that traditional Chinese medicine (TCM) has significant advantages in the comprehensive treatment and regulation of multi-target diseases. IS involves multiple mechanisms, and many studies have shown that some TCM and naturally derived compounds exert protective effects on IS with few side effects[20,21]. Additionally, TCM could alter the relative abundance of gut microbiota and their therapeutic effect was at least partially due to their ability to regulate gut microbiota[12]. *Panax notoginseng* (Burk) F. H. Chen, a kind of TCM was widely used for thousands of years in China to promote blood circulation and remove blood stasis. Its main bioactive ingredients are *P. notoginseng saponins* (PNS)[22]. PNS has been clinically used in the treatment of IS in China for decades of years due to its neuroprotective effects[23]. Our previous data roughly indicated that PNS had a long half-life in the intestines of rats and exhibited significant mutual regulation with gut bacteria, and pre-administered PNS exerted neuroprotective effects *via* regulating gut microbiota disruption[24]. Moreover, our findings also revealed that *Lactobacillus* was the microbiota most profoundly affected by ischemia/reperfusion (I/R) modeling. Rb1, the highest content saponin component in PNS, exerted a significant therapeutic effect on IS *via* regulating gut microbiota and then reversing the accumulation of branched-chain amino acids caused by IS[25]. However, the molecular mechanism and target of action of PNS on IS are not fully understood yet.

The primary purpose of the present study was to identify target microbiota and their metabolites associated with IS and then further reveal the molecular mechanism and target of PNS therapy for IS. To narrow the gap between preclinical and clinical studies, we first searched for small molecule metabolites related to stroke

in the serum of stroke patients. Notably, serum samples from clinical IS patients were divided into acute and obsolete IS groups. Due to the gradual recovery of the I/R model rats after 2 days of modeling, we innovatively designated the rats from 0 to 2 days after modeling as the acute phase and from 3 to 14 days as the rehabilitation phase. Metabolomics analysis showed a significant reduction in serum HIS exposure in both clinical obsolete IS patients and preclinical rehabilitation period I/R rats. PNS could increase the exposure of HIS in I/R rats by up-regulating the proportion of *L.Reu*, thereby significantly increasing the level of intracerebral HA and exerting therapeutic effects on IS. Thus, our results innovatively revealed the role of *L.Reu*-mediated HIS metabolism in the pathogenesis and treatment of IS.

2. Materials and methods

2.1. Animals and treatments

Male Sprague−Dawley rats, weighing 200−230 g and aged 6 weeks, were purchased from Shanghai Super-B&K Laboratory Animal Corp., Ltd. (SCXK2013-0016; Shanghai, China). The rats were housed under controlled conditions, with a temperature of 25 °C, humidity between 55%−60%, a 12/12 h light/dark cycle, and free access to food and water. After a 5-day acclimation, rats were randomly divided into different groups and all animal experiments were approved by the Institutional Animal Care and Use Committee of China Pharmaceutical University.

I/R model rats were established following the procedures of middle cerebral artery occlusion combined with reperfusion as previously described[24]. Briefly, after being anesthetized by intraperitoneal injection of 60 mg/kg of zoletil and 10 mg/kg of xylazine, the left common carotid artery, internal carotid artery, and external carotid artery were surgically exposed *via* a midline incision in the neck. A silicone rubber-coated filament with an external diameter of 0.28 mm was carefully inserted into the internal carotid artery to a depth of approximately 18−21 mm through the stump of the external carotid artery, effectively occluding the left middle cerebral artery. Following a 2 h period of middle cerebral artery occlusion, the occluding filament was gently withdrawn to restore blood flow. Rats in the control group underwent the same surgery except for ligating the carotid artery. Rats within the first 2 days after modeling were designated as being in the acute phase, while those from 3 to 14 days after modeling were designated as being in the rehabilitation phase. I/R+PNS rats were orally administered 100 mg/kg of PNS for 7 consecutive days and rats in the control and I/R groups were given the same volume of saline. Monitoring of body weight and neurological assessments were conducted per day.

The pseudo-germ-free (GF) rats were established *via* intragastric administration of combined antibiotics (including 100 mg/kg of streptomycin sulfate and 100 mg/kg of neomycin sulfate) for 7 consecutive days before I/R modeling. The control group rats were given the same volume of saline.

To construct vagotomy rats, SD rats were anesthetized and fixed on the operating table after the disappearance of the eyelid reflex. A transverse incision of approximately 2 cm was cut beneath the xiphoid process of the sternum. Ligaments surrounding the stomach and mesentery were detached, and the stomach was pulled to the abdominal surface. Subsequently, the gastric branches of the bilateral vagus nerve were cut off, and the abdominal cavity was washed with sterile physiological saline at 37 °C after surgery.

2.2. Neurological severity scores (NSS)

The neurological function of rats was scored on a 5-point scale every two days from I/R modeling until the rats were euthanized: 0 point indicates that the rat has no symptoms of nerve damage; 1 point indicates mild nerve damage and rats cannot fully extend their contralateral forepaws; 2 point indicates moderate nerve damage, with symptoms of rats rotating towards the paralyzed side; 3 point indicates severe nerve damage, with symptoms of rats tilting towards the opposite side; 4 point indicates extremely severe neurological damage, with symptoms of rats being unable to walk and losing consciousness spontaneously.

2.3. Enzyme-linked immunosorbent assay

After rats were euthanized on Day 7 after modeling, the levels of intracerebral inflammatory factors (TNF-α, IL-1β, and IL-6) were measured using the enzyme-linked immunosorbent assay according to the manufacturer's instructions (ExCell Biology, Shanghai, China).

2.4. Triphenyl tetrazolium chloride (TTC) staining

After rats were euthanized on Day 7 after modeling, cerebral infarct size was assessed using TTC staining assay. The rat brain tissue was sectioned into 2-mm-thick slices and immersed in 0.1% TTC staining. After incubating at 37 °C for 30 min, normal brain tissue appeared red, while infarcted slices appeared white. After fixing with 4% paraformaldehyde for 24 h, photos were taken and image processing was performed using Adobe Photoshop 7.0 software. Image-J software was used to calculate the infarct volume.

2.5. Immunofluorescence labeling of neurons

After rats were euthanized on Day 7 after modeling, the rat brain was dehydrated and cut into 50 μm slices. Then the slices were blocked in 3% Triton X-100 and 5% BSA followed by incubating overnight with the mouse anti-neuronal nuclei antigen (Abcam, USA). Then, the slices were washed 3 times with PBS and incubated with a second antibody with anti-mouse IgG (Abcam, USA). Lastly, the slices were placed on a microscope slide for imaging.

2.6. Culture of oxygen-glucose deprivation/reoxygenation (OGD/R)-hCMEC/d3 cells

The hCMEC/d3 cells were purchased from Nanjing Lixing Biotechnology Co., Ltd. (Nanjing, Jiangsu, China), and cultured in Dulbecco's modified Eagle's medium (DMEM) containing 10% fetal bovine serum, 100 U/mL of penicillin, and 100 μg/mL of streptomycin. When the cells reached 80%−90% confluence, they were seeded into a 96-well plate at a density of 8×10^3 cells/mL. Following an overnight cultivation of 12 h, OGD modeling was initiated. During this procedure, the cells were washed with fresh serum-free and sugar-free DMEM medium 3 times, and serum-free and sugar-free DMEM medium was added to the cell plate for cultivation in a low oxygen chamber (1% O_2, 5% CO_2 and 94% N_2). After 12 h, the cells were reoxygenated in serum-free

DMEM containing 30 μg/mL of PNS for 1 h in an incubator. The viability of cells was assessed using CCK-8.

2.7. 16s rRNA sequencing of intestinal microbiota

Genomic DNA of intestinal flora was extracted using E.Z.N.A.® Soil DNA Kit (Omega Bio-Tek, Norcross, GA, USA), and then diluted to 1 ng/μL using sterile water. The targeted sequencing regions (16SV4/16SV3/16SV3-V4/16SV4-V5) were amplified using specific primers. The PCR products, extracted from a 2% agarose gel, were detected and quantified using the QuantiFluor™-ST blue fluorescence quantification system (Promega Corporation, USA), and then mixed in corresponding proportions according to the sequencing requirements. The construction of libraries was executed using the TruSeq DNA Sample Prep Kit (Illumina, San Diego, CA, USA). Finally, purified amplicons were paired-end sequenced on an Illumina MiSeq platform. The paired-end reads obtained from Miseq sequencing were initially concatenated based on their overlap relationships. After sequence quality control and filtering, operational taxonomic unit clustering analysis and species classification analysis were performed to identify changes in gut bacteria between different populations.

2.8. Quantitative PCR (qPCR) analysis

Gut microbiota DNA was extracted according to the instructions of the Fecal Genome Extraction Kit (Solarbio, Beijing, China). Subsequently, mRNA was reverse transcribed into cDNA using a 5 × PrimeScript™ RT Master Mix (4 μL), total RNA (2 μL), and RNase Free dH_2O (14 μL). The following qPCR system was as follows: SYBR Green (7.5 μL), PCR forward primer (6 μmol/L , 1 μL), PCR reverse primer (6 μmol/L, 1 μL), cDNA (1 μL), RNase Free dH_2O (4.5 μL). Specific primer sequences were provided in Supporting Information Table S1. The reaction conditions consisted of a pre-denaturation step at 95 °C for 90 s, followed by a PCR cycle (95 °C for 30 s, annealing temperature 60 °C for 30 s, 72 °C for 30 s) repeated for 40 cycles. A dissolution curve analysis was conducted by heating from 65 to 95 °C at intervals of 0.5 °C/5 s.

2.9. In vitro incubation of gut microbiota with PNS

After gavage administration of PNS to I/R rats for 7 consecutive days, the ileocecal valve contents of control and I/R rats were collected and transferred to sterile 10 mL tubes. After adding 5 times the volume of sterile PBS, homogenize the content and let it stand for 20 min until the food residue settles at the bottom. Next, a six-well plate was prepared and each well was added with 0.3 mL of ileocecal valve content supernatant, 2.1 mL of anaerobic mercaptoacetate medium, and 0.6 mL of PBS containing PNS (0, 10 (L), or 20 (H) mg/mL). Then, the culture medium of different groups was collected at 0 and 12 h during the incubation in a 37 °C anaerobic chamber for subsequent HIS concentration analysis.

2.10. Culture and inoculation of L.Reu

The freeze-dried powder of *L.Reu* (CICC 6226) was purchased from the China Industrial Microbial Strain Collection and Management Center (CICC, Beijing, China). The *L.Reu* powder was suspended in sterile Reinforced Clostridial Medium culture medium, and subsequently cultured in de Man, Rogosa, and Sharpe broth (MRS broth, Difco) at 37 °C for 12 h. To fully restore the bacteria vitality, *L.Reu* was placed in an anaerobic incubator for cultivation and subjected to inoculation for 2−3 generations. I/R+*L.Reu* rats were orally administered 1 mL of *L.Reu* (10^9 CFU/mL) for 7 consecutive days, and daily weight measurements and behavioral assessments were conducted. Serum and brain tissue were collected on the 8th day.

2.11. Metabolomic analysis of clinical and preclinical serum samples

To identify clinical target metabolites related to IS, we collected clinical serum samples from 48 healthy volunteers, 67 acute stroke patients, and 94 obsolete stroke patients. The study was approved by the Affiliated Hospital of Nanjing University of Chinese Medicine in Jiangsu Province ethics committee on June 07, 2018 (ethics number of 2018NL-048-02, approval document was shown in Supporting Information Fig. S1). All participants provided written informed consent. The serum specimens were stored at −80 °C before use. As to preclinical samples, the serum of rats in Control, I/R, and I/R+PNS groups was collected at 24 h (acute phase) and Day 7 (rehabilitation phase) after modeling.

In the pre-treatment process, 200 μL of methanol containing ^{13}C-glutamine (internal standard) was added to 50 μL of serum to precipitate protein. The supernatant was concentrated and evaporated under vacuum, followed by re-dissolved in 200 μL of ultrapure water for analysis. The metabolites were eluted onto an XBridge® Amide column (3.5 μm, 4.6 mm × 100 mm, Waters) and separated using the gradient elution program on Shimadzu UFLC-30A system (Shimadzu, Kyoto, Japan). The aqueous mobile phase was H_2O:CH_3CN 19:1 (*v*/*v*), containing 0.1% ammonium acetate (5 mmol/L) and 0.015% ammonia. The organic mobile phase was CH_3CN. Metabolomics was analyzed using ESI in negative ion mode on AB SCIEX 5600 Q-TOF MS system. The mass spectrometer (MS) operated at the following parameters: Gas1, 33 psi; Gas 2, 33 psi; Curtain Gas, 25 psi; ionic atomization voltage, −4500 V; ion source temperature 550 °C; TOF MS^1 scan, 50−1000 *m/z*; IDA scanning, 50−900 *m/z*; CE, −20 V; CES, 10; DP, −93 V. In the data processing process, Formula Predictor software was used to predict the molecular formula of the compounds. Meanwhile, all the metabolites were identified with the aid of MASSBANK, METLIN, and MS2T databases. Quantitative analysis was conducted using MultiQuant 3.0 software. Multivariate data analysis and modeling were accomplished using Metaboanalyst software.

2.12. Quantitative analysis of HIS and HA in biological samples

In 50 μL of serum or brain homogenate, 5 μL of 2,5-dihydroxybenzoic acid was added as the internal standard, and 150 μL of acetonitrile was added to precipitate protein. The supernatant (5 μL) was injected into LC−MS/MS system for quantitative analysis. Chromatographic separation was performed on an XBridge® Amide column (3.5 μm, 4.6 mm × 100 mm, Waters) under a gradient elution program mode. The aqueous mobile phase was H_2O containing 0.1% HCOOH and 1 mmol/L of $HCOONH_4$. The organic mobile phase was acetonitrile, and the total flow rate was 0.4 mL/min. The MS was operated using ESI spray in positive ion mode. The parameters for HIS were as follows: MRM transition, 156.0 → 110.1 (*m/z*); CE, −21.0 eV; Q1 deviation, −15.0 V; Q3 deviation, −21.0 V. The MS parameters

for HA were as follows: MRM transition, 112.1 → 95.1 (*m/z*); CE, −25.0 eV; Q1 deviation, −16.0 V; Q3 deviation, −17.0 V. The internal standard was detected under the following parameters: MRM transition, 153.1 → 108.2 (*m/z*), CE, 26.0 eV; Q1 deviation, 23.0 V; Q3 deviation, 19.0 V.

2.13. MS imaging (MSI) analysis of intracerebral HIS on DESI XS-Xevo TQ absolute system

Brain tissues were sectioned into 10 μm thickness using a Leica CM1950 slicer, and then mounted onto glass slides. Targeted MSI experiments were carried out on a DESI XS-Xevo TQ Absolute system, which is equipped with a desorption electrospray ionization (DESI) source combining a MS/MS analyzer (Waters, Milford, MA, USA). The spray solvent was methanol/water/formic acid (98:2:0.01, *v/v/v*, 2.0 μL/min). The MRM transition for HIS was 156 → 110 (*m/z*) in positive mode. The capillary voltage, cone voltage, and temperatures of heated transfer line were set to 0.7 kV, 25 V, and 250 °C, respectively.

2.14. Culture of OGD/R-PC12 cells

PC12 cells were purchased from the ATCC cell bank and cultured in DMEM medium containing 10% fetal bovine serum, 100 U/mL penicillin, and streptomycin. To construct the OGD/R cell model, the passaged PC12 cells were initially cultured in DMEM medium containing 10% fetal bovine serum for 12 h. Following cell adhesion, they were transferred to glucose-free DMEM and placed in a low oxygen chamber (1% O_2, 5% CO_2, and 94% N_2) for another 12 h. Then, under normal oxygen conditions, the cells were reoxygenated in DMEM containing glucose for 12 h. During cell hypoxia and reoxygenation, 0.1−1 μmol/L HA or 0.1−10 mmol/L HIS was added to the culture medium to investigate the pharmacological activities of HA and HIS. The viability of cells was assessed using CCK-8.

2.15. Cell apoptosis assay

PC12 cells (1.5×10^4 per well) were seeded in a 6-well plate, and subjected to OGD/R modeling. The cells were then collected, centrifuged, resuspended, and counted. Approximately 5×10^4 to 1×10^5 resuspended cells were incubated with a solution containing Annexin V-FITC and propidium iodide. After a 20 min incubation at room temperature, cell apoptosis was measured using AccuriC6 flow cytometry (Becton Dickinson, USA), and the BD Accuri C6 software was employed to calculate the proportion of cell apoptosis.

2.16. qPCR analysis of intracellular inflammatory cytokines

PC12 cells were seeded in a 6-well plate at a density of 1.5×10^4 per well. After OGD/R molding, 400 μL of Trizol was added to lyse cells. RNA extraction, reverse transcription, and cDNA synthesis were performed according to the instructions. In the PCR plate, cDNA (1 μL), forward prime (1 μL), reverse prime (1 μL), SYBR (7.5 μL) and DEPC water (4.5 μL) were added. Specific primer sequences were provided in Table S1. The ABI Prism 7500 HT sequence detection system was used to detect CT values and calculate relative expression levels.

2.17. Measurement of intracellular reactive oxygen species (ROS)

Oxidative stress was assessed by measuring intracellular ROS levels using the 2′,7′-dichlorofluorescein diacetate (DCFH-DA) staining assay. Briefly, PC12 cells were seeded in 96-well plates at a density of 1×10^4 cells per well. After OGD/R molding, the cells were washed with sterilized PBS, and incubated in serum-free DMEM containing 10 μmol/L DCFH-DA for 1 h at 37 °C. Following three washes with PBS, images were captured using laser scanning confocal microscopy. The fluorescence intensity of ROS was quantified using a multifunctional fluorescence microplate reader, with excitation and emission wavelengths set at 488 and 525 nm, respectively.

2.18. Statistical analysis

All the results were presented with mean ± standard deviation (SD) of 6−7 rats per group using GraphPad Prism 8 software (GraphPad, RRID: SCR_002798). Statistical significance was assessed using Student's *t*-test for two-group comparisons. For multiple-group comparisons, parametric ANOVA was employed only when $F < 0.5$. In instances where results were presented relative to the control, non-parametric ANOVA was conducted. Values of $P < 0.05$ were considered statistically significant.

3. Results

3.1. Therapeutic effect of PNS on IS

To investigate the therapeutic effect of PNS on IS, I/R model rats were established and orally administrated with PNS at a dose of 100 mg/kg for 7 consecutive days. As shown in Fig. 1A, PNS administration significantly alleviated the gradual weight loss caused by I/R modeling. Besides, PNS could considerably reverse the deterioration of NSS in I/R rats (Fig. 1B). Meanwhile, I/R modeling significantly up-regulated the levels of intracerebral pro-inflammatory factors, including TNF-α, IL-1β, and IL-6. PNS in turn significantly reversed the elevation of these pro-inflammatory factors (Fig. 1C−E). Furthermore, the results of TTC staining of brain tissues demonstrated that PNS treatment could reduce cerebral infarction from 35% to around 22.0% (Fig. 1F and G). Immunostaining for neuronal nuclei was then employed, revealing a significant improvement in neuronal loss in PNS-treated rats compared to I/R model rats (Fig. 1H and I). To investigate the *in vitro* effects, OGD/R was induced in hCMEC/d3 to simulate IS. Three different concentrations (10, 20, and 50 μg/mL) of PNS were incubated with OGD/R-hCMEC/d3 for 12 h, and cell viability was determined by CCK-8 assay. The results showed that the protective effect of PNS on hCMEC/d3 diminished when the concentration was below 10 μg/mL or above 50 μg/mL (Fig. 1J). We also conducted the same protocol on OGD/R-PC12 cells to validate the effect of PNS and the result was similar (Supporting Information Fig. S2E). Obviously, the protective effect of PNS on PC12 cells was poor, and the survival rate of PC12 cells could only be improved when the concentration reached 10 μg/mL. Importantly, considering the low bioavailability of the main saponins of PNS, their exposure level in systemic circulation might not reach pharmacological concentrations[24,26]. Therefore, the therapeutic effect of PNS on IS might not be direct, but rather achieved through indirect peripheral regulation.

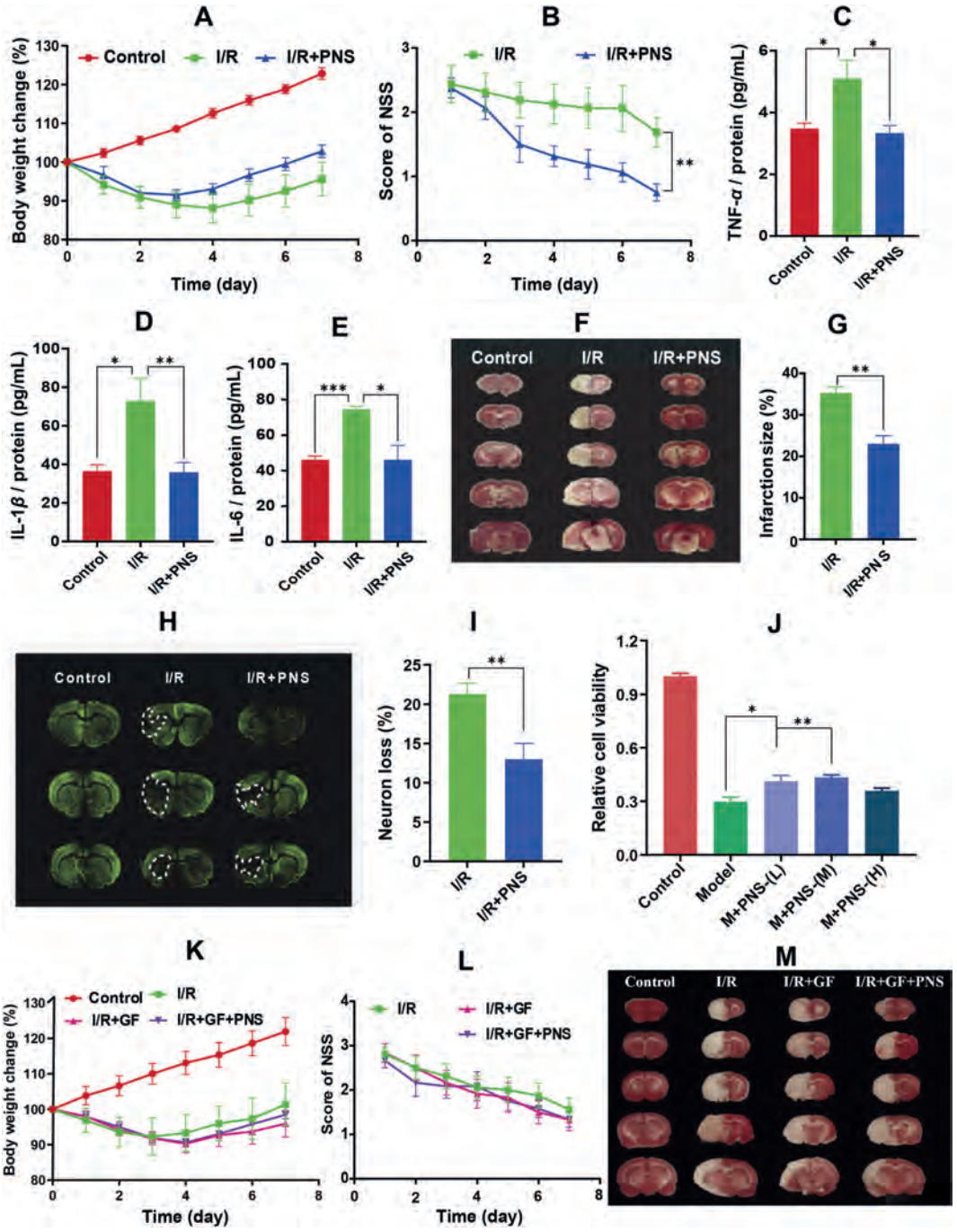

Figure 1 The therapeutic effect of PNS on IR-induced IS in rats. Rats were randomly divided into three groups ($n = 6-7$). I/R+PNS group rats were orally administrated daily with 100 mg/kg of PNS for 7 consecutive days after modeling. Rats in the Control and I/R groups were given the equal volume of saline. (A) Body weight change (%) in Control, I/R, and I/R+PNS groups ($n = 6-7$). (B) NSS in different groups ($n = 6-7$). Intracerebral levels of (C) TNF-α, (D) IL-1β, and (E) IL-6 ($n = 6$). (F) Representative coronal sections of triphenyl tetrazolium chloride (TTC)-stained brains in different groups ($n = 4$). (G) The size of infarction area ($n = 4$). (H, I) Immunofluorescence labeling of neurons in the rat brain of different groups ($n = 4$). (J) Effect of PNS (L: 10 μg/mL, M: 25 μg/mL, and H: 50 μg/mL) on OGD/R-hCMEC/d3 cell viability using CCK-8 assay ($n = 6$). Rats were randomly divided into four groups ($n = 6-7$). I/R+GF and I/R+GF+PNS rats were orally administrated daily with antibiotics for 7 consecutive days before I/R modeling. I/R+GF+PNS rats were orally administrated daily with 100 mg/kg of PNS for 7 consecutive days after modeling. (K) Body weight change (%) in Control, I/R, I/R+GF, and I/R+GF+PNS groups ($n = 6-7$). (L) NSS in different groups ($n = 6-7$). (M) Representative coronal sections of TTC-stained brains in different groups ($n = 4$). ($^*P < 0.05$, $^{**}P < 0.01$, $^{***}P < 0.001$).

Subsequently, the influence of microbiota on the therapeutic effect of PNS on IS was investigated. A pseudo-GF rat model was established by oral administration of combined antibiotics to examine the efficacy of PNS after disrupting gut microbiota. As shown in Fig. 1K and L, the weight loss and NSS among I/R, I/R+GF, and I/R+GF+PNS had no significant difference. However, the combined antibiotics significantly reduced the efficacy of PNS in reducing cerebral infarction area (Fig. 1M and Fig. S2A). Furthermore, PNS could not regulate the enhanced pro-inflammatory factors in the brains of I/R+GF rats (Fig. S2B−S2D). Hence, gut microbiota might exert a crucial role in the treatment of IS with PNS.

3.2. Impact of intestinal microbiota on the treatment of IS

Bacterial community profiling of control, I/R, and I/R+PNS rats was conducted using universal amplification of 16S rRNA gene sequences. Firstly, unweighted uniFrac-based principal coordinates analysis (PCoA) was used to present the microbiota composition in control, I/R, and I/R+PNS rats and the results were shown in Fig. 2A. Compared with the control group, I/R modeling caused the shift in gut microbiota along the direction of PC1 (73.88%). After PNS treatment, the intestinal microbiota migrated to the controls, indicating that PNS had a significant callback effect on I/R-induced microbiota disturbance. Venn plot analysis demonstrated that there were 279 species of common microbiota in the control and model group, 300 species in the control and PNS treatment group, 284 species in the I/R and PNS treatment group, and 263 species common to all three groups (Fig. 2B). Additionally, the unique bacterial communities of control, model, and I/R+PNS groups were 65, 11 and 27, respectively. Therefore, I/R modeling resulted in a decrease in the diversity of gut microbiota, while PNS treatment could dramatically restore the diversity of gut microbiota in I/R model rats. Bar plot analysis was then performed on the gut microbiota profiling, revealing that I/R modeling decreased the abundance of *Firmicutes* and increased the abundance of *Proteobacteria* in the gut microbiota of rats. PNS treatment not only significantly reduced the abundance of *Proteobacteria* in I/R rats but also increased the abundance of *Firmicutes* (Fig. 2C). Notably, analysis of the gut microbiota further indicated that I/R modeling led to a significant down-regulation of *Lactobacilli*, and PNS administration substantially up-regulated *Lactobacillus* levels (Fig. 2D). To further confirm the influence of I/R modeling and PNS administration on *Lactobacilli*, qPCR technology was used for relative quantitative analysis of several common strains of *bacillus,* including *L.Reu, Lactobacillus. Helveticus* (*L.helveticus*), *Lactobacillus. Brevis* (*L.brevis*), and *Bifidobacterium longum* (*B.longum*). Clearly, the proportion of all these *bacilli* in I/R rats was significantly lower than that in sham-operated rats, and PNS intervention markedly up-regulated the proportion of these bacteria. Notably, *L.Reu* was most significantly affected by I/R modeling and PNS administration (Fig. 2E). It aligned with the results obtained from the ANOVA analysis of 16S rRNA data of *L.Reu* (Fig. 2F).

To investigate the effect of *L.Reu* on IS, rats were colonized with 1×10^9 CFU of *L.Reu* for 15 consecutive days after I/R modeling. Then the neuroprotective effects of *L.Reu* were evaluated by comparing the body weight, neurobehavior, infraction size, and intracerebral pro-inflammatory factors of sham-operated, I/R, and I/R+*L.Reu* rats. As shown in Fig. 2G and H, *L.Reu* colonization could dramatically alleviate the weight loss and NSS deterioration caused by I/R modeling. Additionally, *L.Reu* colonization significantly reduced the intracerebral infarction size in I/R rats (Fig. 2I and J). Moreover, colonization of *L.Reu* down-regulated inflammatory factors (TNF-α, IL-1β, and IL-6) in the brains of I/R rats to conventional levels (Supporting Information Fig. S3A−S3C). Therefore, *L.Reu* colonization exerted a significant therapeutic role in I/R cerebral injury.

3.3. Identification of clinical target metabolites related to IS

To identify clinical target metabolites related to obsolete IS, serum specimens were collected from 48 healthy volunteers and 94 patients with obsolete IS for metabolomics analysis. Firstly, differences between the metabolites of two groups were compared using orthogonal partial least squares discrimination analysis (OPLS-DA). As shown in Fig. 3A, there was a distinct separation of serum metabolites between patients with obsolete IS and healthy controls, indicating abnormal small molecule metabolism in patients with IS. The top 25 differential compounds with $P < 0.05$ were then ranked in descending order. Clearly, obsolete stroke resulted in a great reduction in deoxyadenosine monophosphate, HIS and quinoline, while also increasing the exposure of tricarboxylic acid cycle metabolites and amino acids (Fig. 3B). The screened differential compounds were uploaded to Metaboanalyst 5.0 website (https://www.metaboanalyst.ca/) to predict the differential metabolic pathways. Obviously, significant changes occurred in the biosynthesis of aminoacyl groups (HIS, glutamine, cysteine, glycine, methionine, valine, alanine, tyrosine, proline), metabolism of pyrimidine (glutamine, uridine, cytosine nucleoside, deoxycytidine, thymine, thymine), and pentose phosphate pathway in patients with obsolete IS (Fig. 3C). Relative quantitative analysis of small molecule metabolites with significant differences revealed that compared to healthy subjects, HIS levels significantly decreased, while cysteine, alanine, glutamine, tyrosine, proline, and valine accumulated to a certain extent (Fig. 3D).

The metabolome of 67 acute stroke patients and 48 healthy subjects was also analyzed and compared using OPLS-DA. The results showed that there was a marked separation of serum metabolites between patients with acute cerebral infarction and healthy controls (Supporting Information Fig. S4A). Then, the top 25 different compounds were ranked and displayed using heat maps (Fig. S4B). The screened differential compounds were imported into the Metaboanalyst 5.0 website (https://www.metaboanalyst.ca/) to predict the differential metabolic pathways. The bubble size in the bubble chart represented the number of differential metabolites involved in the corresponding pathway, and the bubble color represented the significant difference in *P* value (Fig. S4C). Obviously, the biosynthesis of aminoacyl-tRNA, phenylalanine, tyrosine, and arginine underwent significant alterations when acute IS occurred. We conducted a relative quantitative analysis of small molecule metabolites with significant differences, and the results showed an obvious increase in HIS, phenylalanine, cysteine, glutamate, and isoleucine levels, while the levels of arginine significantly decreased (Fig. S4D).

We also investigated the influence of acute IS on the HIS and HA levels in the I/R model rats (Fig. S4E and S4F). Consistent with clinical results, the serum levels of HIS and HA in rats at 24 h after I/R modeling were significantly higher than those in the sham-operated controls. Similarly, the exposure levels of HIS and HA in rat cortex, striatum, and hippocampus at 24 h after I/R modeling were also significantly higher than those in the controls. Meanwhile, the effect of PNS administration on serum and intracerebral HIS and HA levels was not significant.

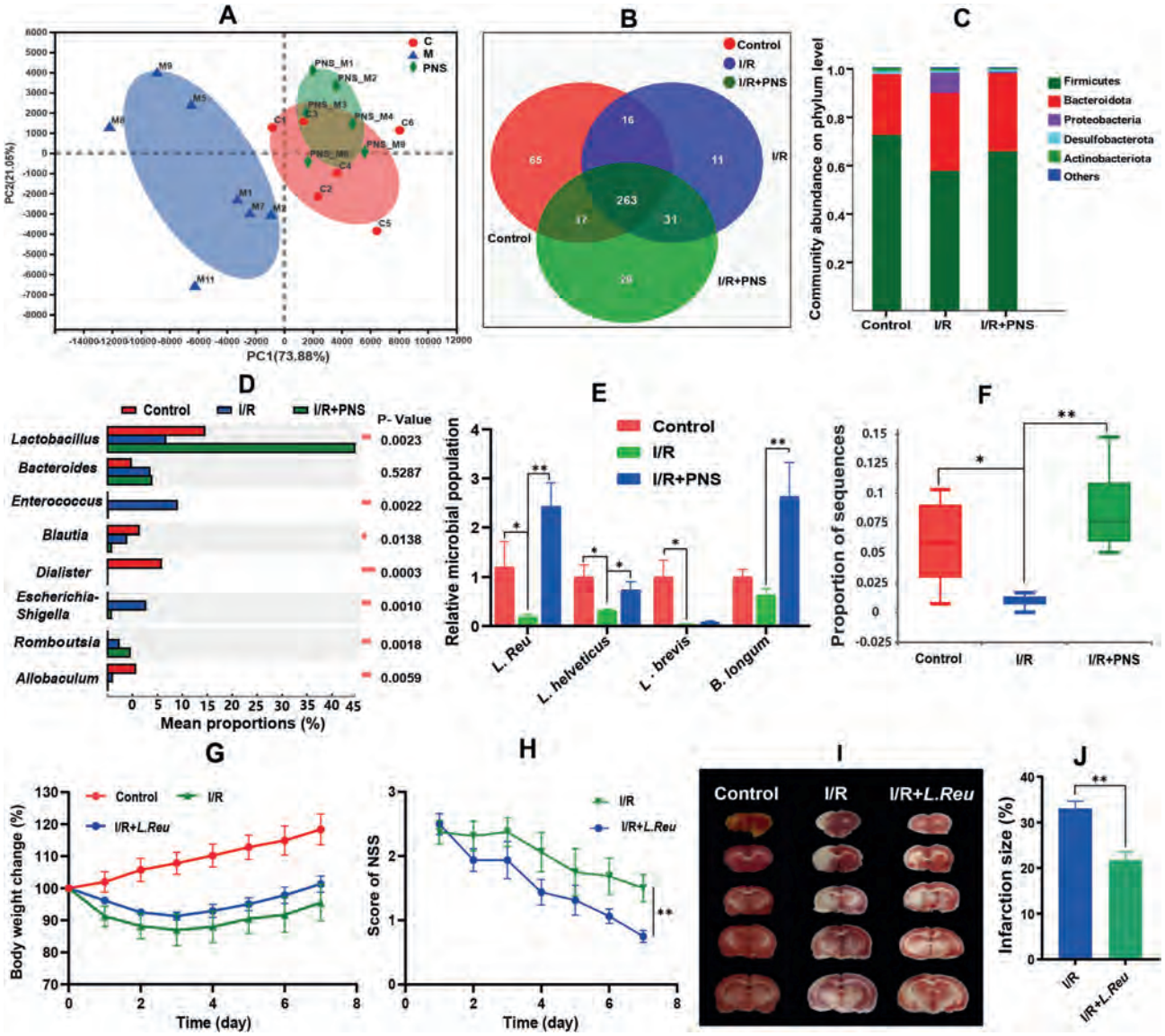

Figure 2 Impact of intestinal microbiota on the treatment of IS. (A) PCoA plot of bacterial Operational Taxonomic Unit in fecal samples of Control, I/R and I/R+PNS rats. Each symbol represents the data of an individual rat ($n = 6-7$). (B) Venn graphs of three experimental groups. (C) Bacterial taxonomic profiling at phylum level in different groups ($n = 6-7$). (D) Mean proportions of significant genus in intestinal microbiota of different groups ($n = 6-7$). (E) Relative population of significant species using qPCR ($n = 6-7$). (F) Proportion of sequences of *L.Reu* using the ANOVA analysis of 16S rRNA data ($n = 6-7$). Rats were randomly divided into three groups ($n = 6$). I/R+*L.Reu* rats were orally administered daily with 1 mL of *L.Reu* (10^9 CFU/mL) for 7 consecutive days after modeling. (G) Body weight change (%) in Control, I/R, and I/R+ *L.Reu* groups ($n = 6$). (H) NSS in different groups ($n = 6$). (I) Representative coronal sections of TTC-stained brains in different groups ($n = 4$). (J) The size of infarction area ($n = 4$). (*$P < 0.05$, **$P < 0.01$).

3.4. Influence of PNS and gut microbiota on the exposure of HIS in rats

Metabolomics studies on clinical specimens suggested that serum HIS levels in patients with obsolete IS significantly decreased, while amino acid content significantly increased. To further confirm the correlation between these small molecule metabolites and IS, the metabolomics studies on rat serum were investigated. PCA results illustrated that the small molecule metabolites in sham-operated and I/R rats at 7 d after I/R modeling were obviously differentiated (Supporting Information Fig. S5). Compared with the control rats, the distribution of small molecule metabolites in I/R rats extended to the lower left quadrant. PNS administration shifted the distribution of metabolites to the upper right quadrant, indicating that PNS administration had a significant callback effect on metabolic abnormalities caused by I/R modeling. Subsequently, the metabolic pathways of differential metabolites were analyzed, and the results demonstrated that I/R modeling and PNS administration could significantly regulate multiple metabolic pathways in rats, including aminoacyl biosynthesis (HIS, phenylalanine, arginine, and glutamine), metabolism of alanine, aspartic acid, and glutamic acid (Supporting Information Fig. S6A). Particularly, glutamine, alanine, and valine were significantly up-regulated after modeling,

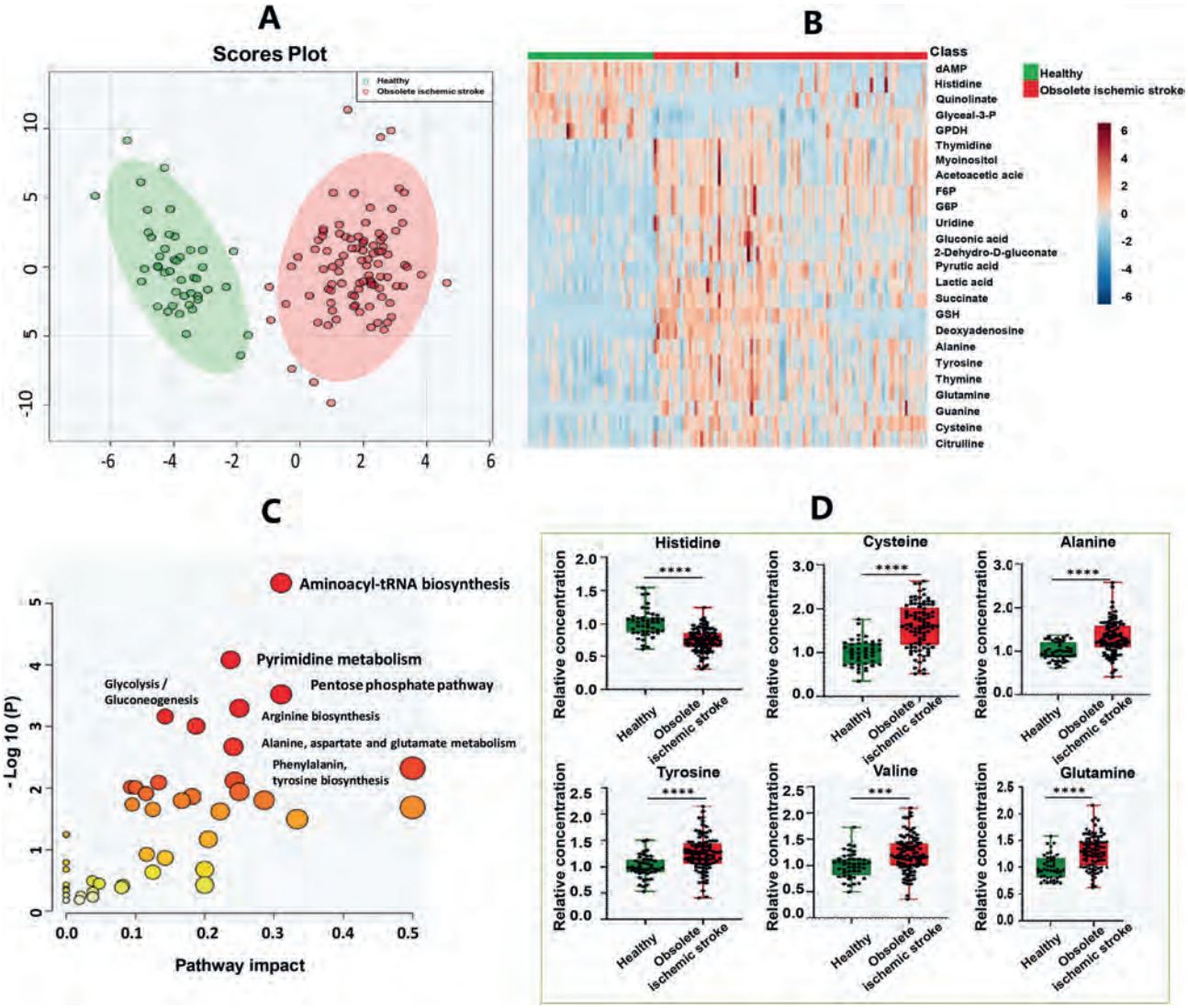

Figure 3 Identification of clinical target metabolites related to obsolete IS. Clinical serum samples from 48 healthy and 94 obsolete stroke patients were collected from Affiliated Hospital of Nanjing University of Chinese Medicine in Jiangsu Province (ethics number: 2018NL-048-02). (A) OPLS-DA analysis of metabolomics in serum samples of healthy and obsolete stroke patients. (B) Heatmap analysis of metabolomics. (C) Analysis of metabolic pathways. (D) Representative differential metabolites. (***$P < 0.001$, ****$P < 0.0001$).

and were effectively recalled after PNS intervention (Supporting Information Fig. S7). Serum HIS levels in I/R rats were significantly lower than those observed in controls, which was consistent with clinical metabolomics. Meanwhile, PNS administration could significantly regulate small molecule metabolic abnormalities caused by I/R modeling, especially in the regulation of HIS. Then, the relative quantitative analysis of HIS levels in the ischemic (left) and normal (right) brain regions of I/R model rats was performed using DESI XS-Xevo TQ Absolute MS system. As shown in Fig. S6B, HIS was uniformly distributed in both the left and right brains of the sham-operated rats. In contrast, the ischemic area indicated by blue dashed lines in optical image, particularly in the neocortex and thalamus of I/R rats, closely matched the region in MS image, with HIS levels significantly lower than non-ischemic regions (Fig. 4A). Consequently, I/R modeling resulted in a decrease in intracerebral HIS exposure. Furthermore, the serum exposure of HIS in sham-operated, I/R, and I/R+PNS rats underwent quantitative analysis using LC−MS/MS. The results demonstrated a reduction in serum HIS levels due to I/R modeling, whereas PNS administration exhibited a significant reversal of the decline in serum HIS (Fig. 4B). Additionally, I/R modeling prompted a decrease in HIS levels in rat cortex, striatum, and hippocampus, and PNS administration could significantly callback intracerebral HIS (Fig. 4C).

HA, a metabolite formed by decarboxylation of HIS, could be generated by various types of cells and gut bacteria[27]. Similar to HIS, the reduction of HA levels in the cortex, striatum, and hippocampus of I/R model rats could be significantly enhanced by PNS administration (Fig. 4D). To explore the mechanism of PNS regulating HIS, we incubated PNS with gut microbiota collected from sham-operated and I/R rats, respectively. As shown in Fig. 4E and F, PNS could increase the production of HIS in intestinal bacteria in a dose-dependent manner. Additionally, exogenous PNS significantly increased HIS exposure in the ileocecal valve of rats (Fig. 4G). HIS decarboxylase (HDC) is a key rate-limiting enzyme for the conversion of HIS to HA. HDC was

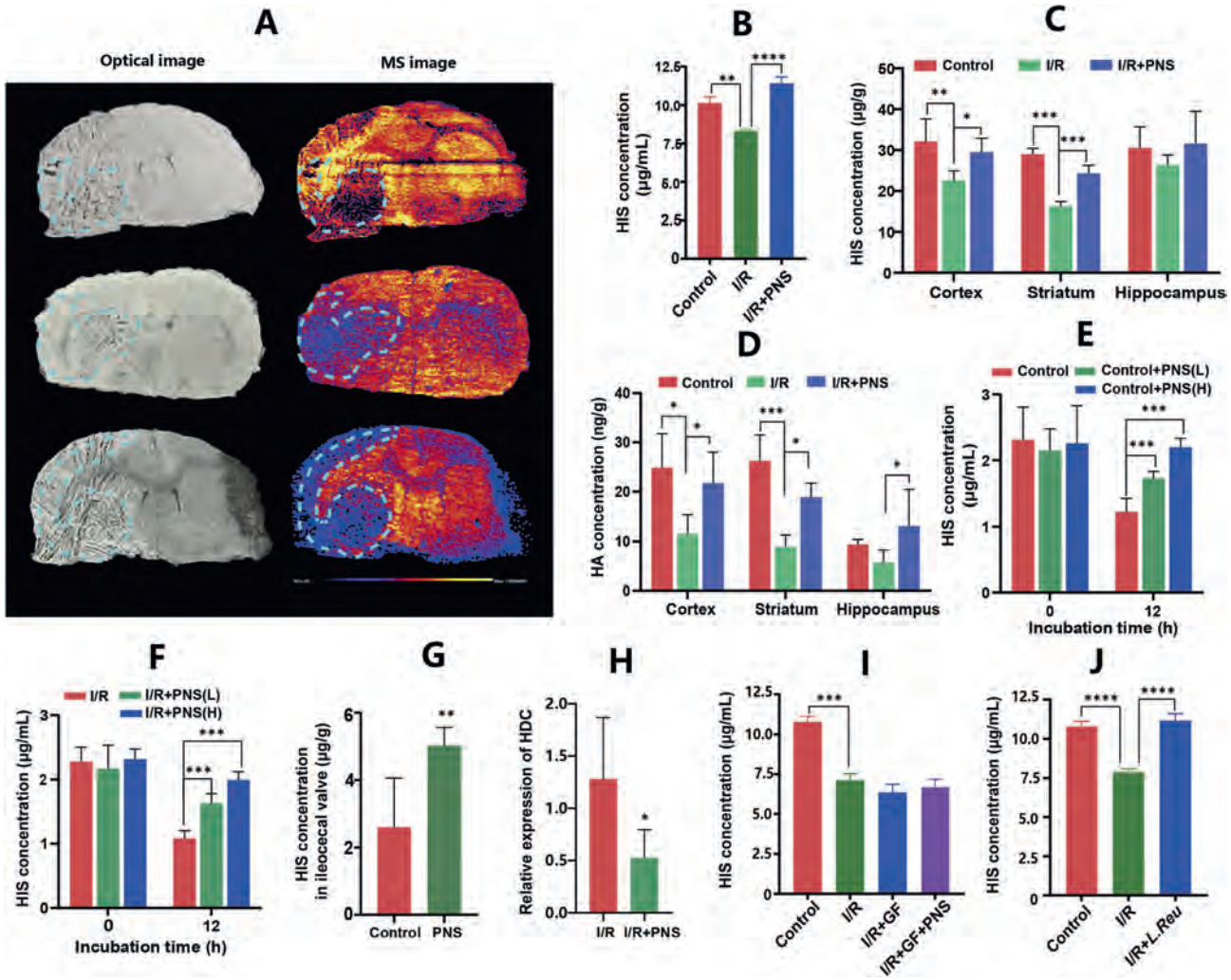

Figure 4 Influence of PNS and gut microbiota on the exposure of HIS in rats. (A) Optical image (left) and MSI imaging (right) of intracerebral HIS of I/R rat brain slices ($n = 3$). The areas shown with blue dashed lines in optical and MS images are areas that had cerebral ischemic infarction and low HIS levels. (B) HIS levels in the serum of Control, I/R, and I/R + PNS rats ($n = 6$). (C) HIS and (D) HA levels in the cortex, striatum, and hippocampus of different groups ($n = 6$). HIS levels in the incubation system of gut microbiota collected from (E) Control and (F) I/R rats at 0 and 12 h ($n = 4$). (G) HIS level in the ileocecal valve of rats ($n = 6$). (H) Relative expression of HDC in the ileocecal valve of rats ($n = 6$). (I) HIS levels in the serum of Control, I/R, I/R+GF and I/R+GF+PNS rats ($n = 6$). (J) HIS levels in the serum of Control, I/R, and I/R+ *L.Reu* rats ($n = 6$). (*$P < 0.05$, **$P < 0.01$, ***$P < 0.001$, ****$P < 0.0001$).

not only present in mast cells and gastrointestinal chromaffin cells, but also in the gut microbiota. To investigate the regulatory mechanism of PNS on intestinal HIS, we extracted total genomic DNA from the ileocecal valve content and performed qPCR analysis on the expression of HDC. Clearly, exogenous PNS significantly down-regulated the expression of HDC in the ileocecal valve of I/R model rats (Fig. 4H). Therefore, exogenous PNS could significantly reduce the conversion of HIS to HA, thereby increasing the exposure level of HIS in the gut microbiota. More importantly, we further confirmed the influence of gut microbiota on HIS by examining the regulatory effect of combined antibiotics and *L.Reu* colonization on rat serum HIS. It was found that once combined antibiotics were used to disrupt the gut microbiota, the regulatory effect of PNS on HIS disappeared (Fig. 4I). Colonization of *L.Reu* could also greatly enhance the serum HIS level in I/R rats (Fig. 4J).

3.5. Effect of HA and HIS on cerebral infarction in OGD/R-PC12 cells

OGD/R-PC12 cells were used as an *in vitro* model for simulating cerebral infarction. In OGD/R-PC12 cells, the effect of HIS and HA on cerebral infarction was investigated *via* measuring the levels of apoptosis and inflammatory factors. As shown in Fig. 5A and Supporting Information Fig. S8A, OGD/R modeling significantly increased the apoptosis rate of PC12 cells from 8.14% to 15.58%. The administration of 0.5 and 1 μmol/L of exogenous HA could reduce the apoptosis rate to 10.03% and 7.72%, respectively. Additionally, exogenous HA could also enhance the viability of OGD/R-PC12 cells in a dose-dependent manner (Fig. 5B). Furthermore, OGD/R modeling resulted in an up-regulation of TNF-α, IL-6, and IL-1β by 3.7-, 2.4- and 2.7-fold, respectively. Exogenous HA could dose-dependently restore the

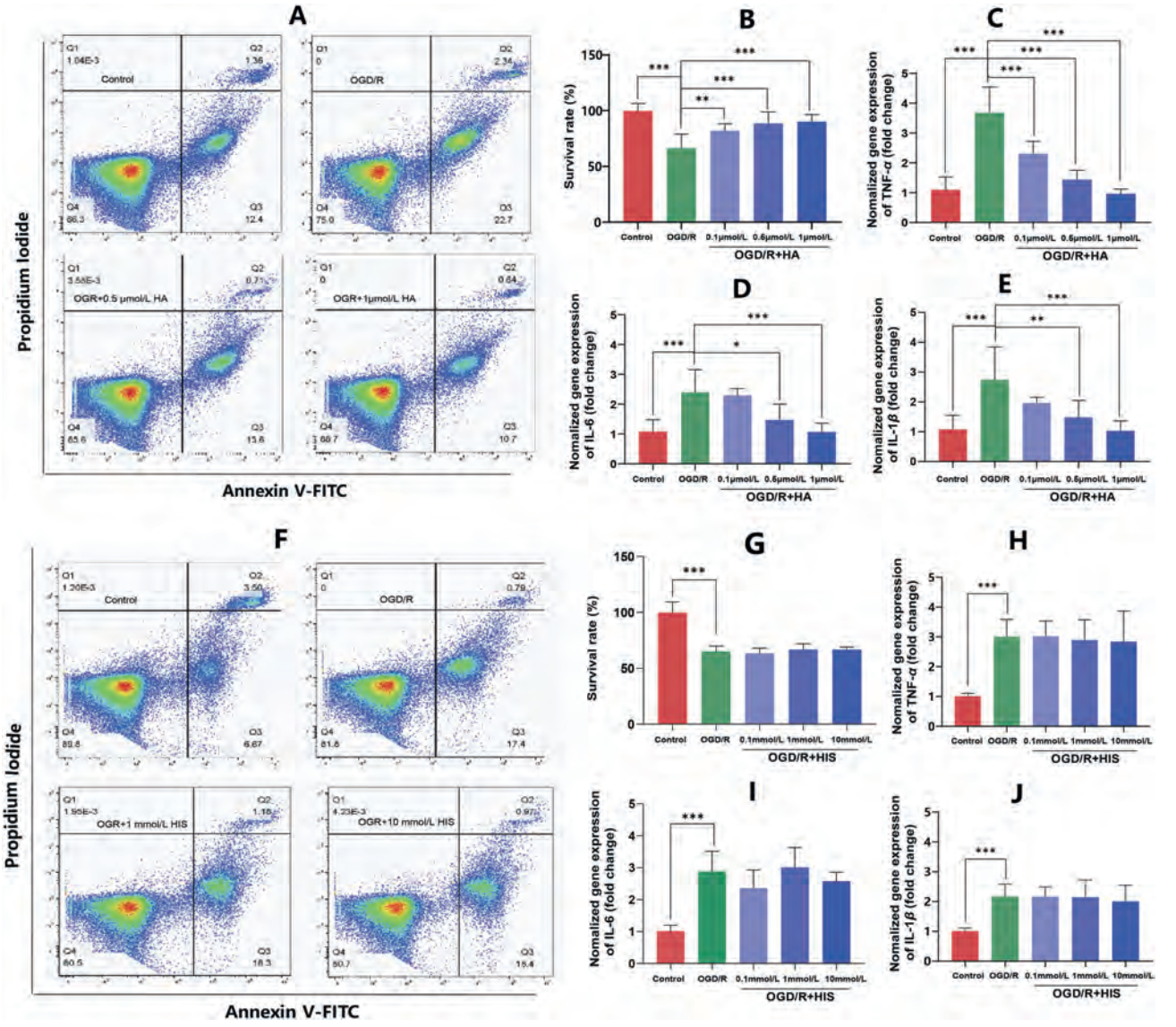

Figure 5 Effect of HA and HIS on cerebral infarction in OGD/R-PC12 cells. (A) Influence of HA (0.5 and 1 μmol/L) on the apoptosis of OGD/R-PC12 cells ($n = 6$). (B) Influence of HA (0.1, 0.5, and 1 μmol/L) on the survival rate, (C) TNF-α, (D) IL-6, and (E) IL-1β of OGD/R-PC12 cells ($n = 6$). (F) Influence of HIS (1 and 10 mmol/L) on the apoptosis of OGD/R-PC12 cells ($n = 6$). (G) Influence of HIS (0.1, 1, and 10 mmol/L) on the survival rate, (H) TNF-α, (I) IL-6, and (J) IL-1β of OGD/R-PC12 cells ($n = 6$). (*$P < 0.05$, **$P < 0.01$, ***$P < 0.001$).

expression of inflammatory factors in OGD/R-PC12 cells to normal levels (Fig. 5C−E). Therefore, HA exerted an excellent protective effect on PC12 cells damaged by OGD/R. Next, we investigated the effects of HIS on apoptosis, viability, and inflammatory factors in OGD/R-PC12 cells. As shown in Fig. 5F and Fig. S8B, 1 and 10 mmol/L of exogenous HIS could not alleviate the excessive apoptosis. Furthermore, the influence of HIS and HA on oxidative stress was assessed by labeling intracellular ROS with DCFH-DA probe. Clearly, the fluorescence intensity of OGD/R-PC12 cells was much higher and 1 μmol/L of exogenous HA could reduce the intensity (Fig. S8C and S8D). In addition, HIS also could not improve the viability and inflammatory factors of OGD/R-PC12 cells (Fig. 5G−J).

3.6. *Influence of HIS on cerebral infarction in I/R rats*

Published data suggested that HA could alleviate brain damage in cultured neuronal cells and animal models[28]. Our above results also indicated that it is HA rather than HIS that exerts neuroprotective effects. Since HA is generated through HIS decarboxylation metabolism *in vivo*, we investigated the influence of HIS on cerebral infarction in I/R rats. Herein, I/R rats were intragastrically administrated with HIS at a dose of 500 mg/kg for 14 consecutive days to investigate the effect of exogenous HIS on cerebral infarction. Obviously, exogenous HIS could greatly enhance the exposure of HIS in I/R rats (Fig. 6A). HIS administration could also alleviate weight loss caused by I/R modeling

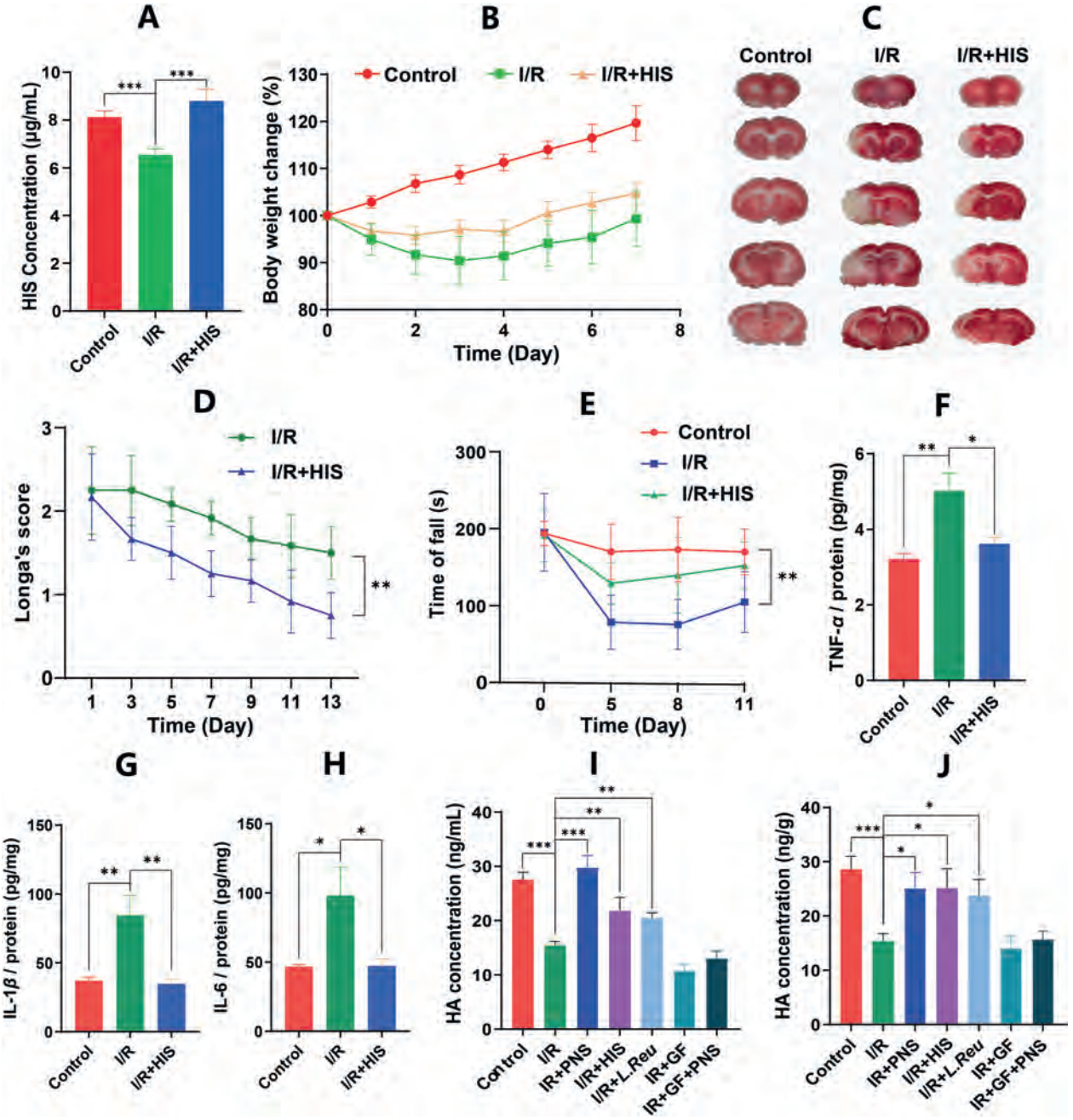

Figure 6 Influence of HIS on cerebral infarction in I/R rats. Rats were randomly divided into three groups ($n = 6$). I/R+HIS rats were orally administrated daily with 500 mg/kg of HIS for 14 consecutive days after modeling. (A) Concentrations of HIS in the rat serum of Control, I/R, and I/R+HIS groups ($n = 6$). (B) Body weight change (%) in different groups ($n = 6$). (C) Representative coronal sections of TTC-stained brains in different groups ($n = 4$). (D) Behavioral score and (E) residence time in the rod rotation test of rats in different groups ($n = 6$). Intracerebral levels of (F) TNF-α, (G) IL-1β, (H) IL-6 ($n = 6$). (I) HA levels in the rat serum ($n = 6$). (J) HA levels in the rat brain ($n = 6$). (*$P < 0.05$, **$P < 0.01$, ***$P < 0.001$).

(Fig. 6B). Cerebral TTC staining demonstrated that exogenous HIS significantly reduced the cerebral infarction area in rats compared to I/R rats (Fig. 6C and Supporting Information Fig. S9A). Longa score was used to evaluate the neurological deficits of rats. As shown in Fig. 6D, all rats were in a state of moderate neurological damage after I/R modeling. Compared with the I/R model rats, HIS administration showed significant improvement, with scores dropping from 2.2 to 0.9. The rotational rod method was used to evaluate the motor ability of rats after I/R modeling. On the 5th day after modeling, the residence time of the I/R rats on the rotating rod decreased to 78 s, while HIS administration significantly prolonged the residence time of I/R rats on the rotating rod to 129 s. With the prolongation of HIS administration time, the improvement of HIS on behavior became increasingly significant (Fig. 6E). Additionally, HIS treatment significantly reversed the rise of intracerebral pro-inflammatory

factors caused by I/R modeling (Fig. 6F−H). Therefore, HIS exerted a significant recovery effect on neural function damage and motor ability in I/R rats.

Since HIS could not prevent damage to PC12 cells caused by OGD/R modeling like its metabolite HA, the conflicting *in vivo* and *in vitro* efficacy suggested that HIS might exert therapeutic effects on IS by converting into HA in I/R rats. Therefore, the influence of exogenous PNS, HIS, and intestinal flora on the exposure of HA was investigated *via* measuring the serum HA of sham-operated, I/R, I/R+PNS, I/R+HIS, I/R+*L.Reu*, I/R+GF and I/R+GF+PNS rats. As shown in Fig. 6I, both PNS and HIS administration could significantly increase serum HA exposure in I/R rats, and *L.Reu* colonization could also enhance the HA level in I/R rats. When the gut microbiota was disrupted by antibiotics, the regulatory effect of PNS administration on HA became insignificant. Notably, both HIS administration and *L.Reu* colonization could significantly increase intracerebral HA exposure in I/R rats (Fig. 6J).

3.7. Role of gut−brain communication in the neuroprotective effect of HIS

Since the gut microbiota mediated the regulation of HA in I/R rats by PNS or HIS, the impact of gut microbiota on the efficacy of exogenous HIS in pseudo-GF model rats was then investigated. Clearly, intragastric administration of exogenous HIS could significantly improve weight loss and NSS scores of I/R+GF rats (Fig. 7A and B). The TTC staining results showed that after I/R modeling, significant cerebral infarction and ischemia occurred in rats, and antibiotics had no significant effect on cerebral infarction. The administration of exogenous HIS to I/R+GF rats significantly reduced the cerebral infarction area (Fig. 7C and D). Additionally, oral administration of exogenous HIS could significantly down-regulate the levels of intracerebral pro-inflammatory factors of I/R+GF rats (Fig. 7E−G). Therefore, HIS could exert a direct neuroprotective effect, which might be independent of the gut microbiota, although the production of HIS was closely related to the gut microbiota.

Emerging evidence suggests that the intestinal microbiota and their metabolites always modulate brain functions directly or indirectly mainly through neuroendocrine hypothalamic pituitary adrenal (HPA) axis, vagal sensory, and peripheral blood pathways (Fig. 7H). The vagus nerve was the main neuronal connection between the intestine and the brain, which could directly send and receive signals between the gut microbiota (and other organs) and the brainstem[6,29]. To further investigate whether the neuroprotective effect of HIS depends on the gut microbiota, we severed the vagus nerve of I/R rats to establish an I/R-vagus composite animal model, and compared the efficacy of HIS on I/R and I/R-vagus model rats. As shown in Fig. 7I and J, administration of exogenous HIS to I/R-vagus rats resulted in a decrease in the proportion of cerebral infarction from 59.93% to 28.65%, and there was no significant difference compared to the I/R + HIS group. The levels of intracerebral inflammatory factors (TNF-α, IL-6, and IL-1β) of I/R-VER+HIS rats were significantly lower than those of I/R rats, and were comparable to the I/R+HIS rats (Fig. 7K−M). After 1 day of I/R modeling, all rats were in a moderate state of neurological damage and vagotomy had no significant effect on the neuroprotection of HIS (Fig. 7N). More importantly, we further investigated the regulatory effects of PNS on HIS and HA in I/R rats after vagotomy. Obviously, intragastric administration of PNS could significantly increase the exposure of HIS and HA in the striatum and cortex of I/R and I/R-vagus rats (Fig. 7O−R). Similarly, exogenous PNS could also enhance the levels of HIS and HA in the hippocampus of both I/R and I/R-vagus rats (Fig. S9B and S9C). Thus, vagotomy did not have a significant effect on the efficacy of HIS, and the enhancement of intracerebral HIS caused by PNS was not achieved through the vagal pathway.

4. Discussion

IS occurs when cerebrovascular diseases disrupt the intracerebral blood supply, causing a significant global burden in terms of mortality and disability[30]. In clinical practice, the current treatment of IS mainly includes thrombolysis and embolization. However, each treatment regime has its own specific limitations, which result in poor treatment outcomes and prognosis for some patients[31]. Therefore, it is urgent to explore new treatment targets and strategies to increase the treatment efficiency of IS. PNS, one of the most valuable Chinese herbal medicines, has been widely used alone or as the key active ingredient of Chinese patent drugs to treat various complicated cases[32]. Our previous data suggested that intragastric administration of PNS before I/R modeling could significantly reduce the severity of cerebral injury by improving dysbiosis in stroke rats[24]. However, the therapeutic effect and mechanism of PNS on IS remain to be further explored.

The main purpose of this study is to provide a novel therapeutic target and strategy for IS based on the pharmacological validation and action mechanism of PNS. In the *in vivo* model, our data demonstrated that PNS treatment could greatly improve the cerebral infarction, NSS, and neuronal loss of I/R rats. In the *in vitro* model, PNS with a concentration of over 10 μg/mL could exert its neuroprotective effect on OGD/R-hCMEC/d3 cells. However, extensive evidence suggests that the bioavailability of the main saponins of PNS was extremely low, and their exposure level in the systemic circulation could not reach the pharmacological concentrations[24,26,33]. Even more ominous is that due to poor permeability, it is difficult for PNS to penetrate the blood-brain barrier[34]. Thus, the pharmacological and pharmacokinetic characteristics of PNS in the treatment of IS were contradictory. The contribution of peripheral regulation in the therapeutic effect of PNS on IS could not be underestimated. Currently, it is generally held that IS would lead to inflammation and immune responses in immune organs such as the brain and intestines[35]. Of particular concern was that IS can cause displacement and alteration of the gastrointestinal microbiota, significantly affecting the severity of brain injury[10]. Nowadays, there has been a significant increase in interest in probiotics considering their abilities to prevent and treat various complex diseases. In particular, the gut microbiota could enhance the exposure and efficacy of TCMs by influencing their pharmacokinetic characteristics. In other words, TCM largely relied on certain specific gut microbiota to exert or enhance their pharmacological effects[12].

Our previous research demonstrated that PNS had a long half-life in the intestines of rats and exhibited significant mutual regulation with gut bacteria[32,36]. Thus, we naturally investigated the impact of gastrointestinal microbiota on the therapeutic efficacy of PNS. Microbial dysbiosis animal model was then established using combined antibiotics and applied to investigate the efficacy of PNS. Unsurprisingly, gastrointestinal dysbiosis significantly weakened the therapeutic effect of PNS on IS. Universal amplification of 16S rRNA gene sequences was used to map bacterial community profile of sham-operated, I/R model and I/R+PNS rats, and the results indicated that I/R modeling led to a significant down-regulation of *Lactobacilli*, and PNS administration could greatly up-regulate

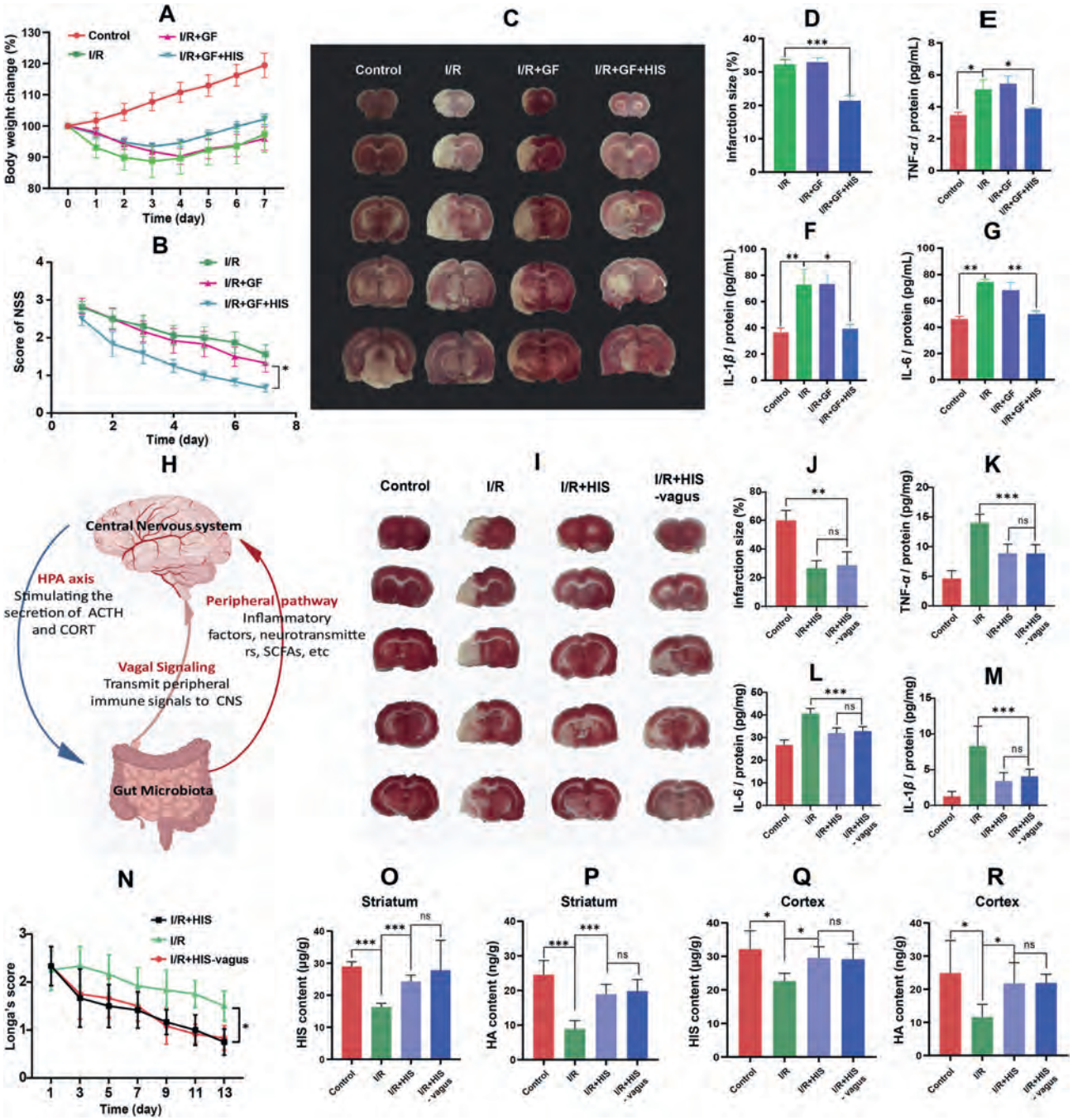

Figure 7 Role of gut−brain communication in the neuroprotective effect of HIS. Rats were randomly divided into four groups ($n = 6$). I/R+GF and I/R+GF+HIS rats were orally administrated daily with antibiotics for 7 consecutive days before I/R modeling. I/R+GF+HIS rats were orally administrated daily with 500 mg/kg of HIS for 14 consecutive days after modeling. (A) Body weight change (%) Control, I/R, I/R+GF, and I/R+GF+HIS groups ($n = 6$). (B) NSS in different groups ($n = 6$). (C) Representative coronal sections of TTC-stained brains in different groups ($n = 4$). (D) The size of infarction area ($n = 4$). Intracerebral levels of (E) TNF-α, (F) IL-1β, and (G) IL-6 ($n = 6$). (H) Pathways of gut−brain axis transmission. Rats were randomly divided into four groups ($n = 6$). I/R+HIS-vagus rats received vagotomy surgery, and I/R modeling was conducted following wound recovery. I/R+HIS and I/R+HIS-vagus rats were orally administrated daily with 500 mg/kg of HIS for 14 consecutive days after modeling. (I) Representative coronal sections of TTC-stained brains in different groups ($n = 4$). (J) The size of infarction area ($n = 4$). Intracerebral levels of (K) TNF-α, (L) IL-6, and (M) IL-1β ($n = 6$). (N) Behavioral score of rats in different groups ($n = 6$). Rats were randomly divided into four groups ($n = 6$). I/R+PNS-vagus rats received vagotomy surgery. I/R+PNS and I/R+PNS-vagus rats were orally administrated daily with 100 mg/kg of PNS for 7 consecutive days after modeling. (O) HIS exposure in the striatum of rats ($n = 6$). (P) HA exposure in the striatum of rats ($n = 6$). (Q) HIS exposure in the cortex of rats ($n = 6$). (R) HA exposure in the cortex of rats ($n = 6$). ($^*P < 0.05$, $^{**}P < 0.01$, $^{***}P < 0.001$).

Lactobacillus levels. Recent clinical trials have found that the frequency of *Bifidobacterium* spp. and *Lactobacillus* spp. in patients with IS has decreased by 2−3 times[37]. Therefore, the target bacterial communities associated with I/R model rats were basically consistent with those of stroke patients. qPCR analysis further revealed that both I/R modeling and PNS administration had the most significant impact on *L.Reu* in *Lactobacilli*. Although the levels of *B.longum* also showed notable changes after PNS administration, there was no significant difference between its levels in the Control and I/R group, implying a closer relationship between *L.Reu* and the pathogenesis of IS. Recent burgeoning literature unveiled that *L.Reu* met all the requirements for safe, well-tolerated, and effective probiotics, and could induce widespread changes in the metabolome and immune system by regulating tryptophan metabolism[38,39]. Herein, I/R model rats were colonized with 1×10^9 CFU of *L.Reu* (CICC6123) for 15 consecutive days to investigate the therapeutic effects of *L.Reu* on IS. Our results demonstrated that *L.Reu* colonization could exert significant neuroprotective effects by improving neurobehavior, infraction size, and intracerebral pro-inflammatory factors.

The gut microbiota contributed to transmitting signals from the gut to the entire system by producing a large amount of metabolic products, thereby promoting the physiological functions of the host[40]. These metabolites served as signaling molecules for metabolic reactions and typically function in several unique modes within the host, which was highly in line with the balance and networked approach of biological regulation[41]. In stark contrast to the dogma of "one gene, one target, one drug", the comprehensive regulatory role of gut microbiota metabolites in coordinating host health can provide a complementary pathway for innovative treatment of chronic and complex diseases[41]. To identify clinical target metabolites related to cerebral infarction, we collected clinical serum samples from 48 healthy subjects, 67 acute stroke patients, and 94 obsolete stroke patients. Metabolomics analysis of healthy volunteers and stroke patients showed a significant decrease in serum HIS levels in obsolete stroke patients. To further confirm the correlation between HIS and IS, we investigated the effect of I/R modeling and PNS administration on serum HIS in rats, and innovatively divided the rats after I/R modeling into two phases (the acute and rehabilitation phases), which correspond to the acute and obsolete IS in the clinics, respectively. The results suggested that HIS levels of rats in serum and brain after 14 days of I/R modeling were significantly lower than those of the controls, which was consistent with the results of clinical metabolomics. Meanwhile, PNS administration could significantly regulate small molecule metabolic abnormalities caused by I/R modeling, especially in the regulation of HIS in the obsolete or rehabilitation phase. Foremost, PNS could increase the production of HIS in an *in vitro* gut microbiota incubation system in a dose-dependent manner, and colonization of *L.Reu* could also greatly enhance the serum HIS level in I/R rats, indicating that *L.Reu* mediated the production of HIS.

Contrary to our findings, some literature reported that stroke induces activation of intestinal mast cells, leading to increased HA secretion and a significant increase in HA levels between 6 h and 7 days after stroke[42,43]. To investigate the reasons for this contradiction, we measured the exposure levels of metabolites in clinical and preclinical samples of acute stroke. Our results revealed that acute cerebral infarction resulted in an aberrant reduction of *N*-acetylomithne, arginine, deoxyuridine, thiamine monophosphate, 6-phosphogluconate, as well as a significant accumulation of malate, citrate, uracil, lactate, taurine, cysteine, phenylalanine, HIS, glutamate, citrulline, and cytidine. Our results showed an obvious increase in HIS, phenylalanine, cysteine, glutamate and isoleucine levels, while the levels of arginine significantly decreased The aberrant accumulation of HIS in patients with acute IS was consistent with previous reports. In addition, we also investigate the influence of acute IS on the HIS and HA levels in the I/R model rats. Consistent with clinical results, the serum and intracerebral levels of HIS and HA in rats at 24 h after I/R modeling were significantly higher than those in the sham-operated controls, and the effect of PNS administration on serum and intracerebral HIS and HA levels was not significant. In sum, we innovatively found that acute stroke leads to abnormal accumulation of HIS and HA, while patients and rats with obsolete stroke have significantly reduced levels of HIS and HA.

HIS has the lowest content of nutritionally essential amino acids in human proteins, and its systemic circulation concentration significantly decreases in chronic obstructive pulmonary disease and chronic kidney disease[44]. HIS levels and supplementation are associated with several health benefits, including but not limited to antioxidants, body weight management, and cognitive improvement[22,45,46]. However, a high intake of HIS (>24 g/day) might lead to adverse reactions such as decreased serum zinc and cognitive impairment. To date, the function of HIS in the progression and treatment of obsolete IS is still unknown. Then the neuroprotective effect of HIS was investigated on OGD/R-PC12 cells and I/R rats. Our results suggested that exogenous HIS (0.1−10 mmol/L) could not alleviate apoptosis and inflammatory damage of OGD/R-PC12 cells, while it exerted a significant recovery effect on neural function damage and motor ability in I/R rats. This contradictory result suggested that the therapeutic effect of HIS on stroke was not its own pharmacological activity. As a major metabolite, HA was once considered a typical inflammatory mediator that can cause Lewis's 'triple reaction' to skin damage *via* H1 and H2 receptors to produce vasodilation and increased vascular permeability[47]. In general, elevated levels of HA were found in inflamed tissue, which was consistent with our results of increased HA levels in acute stroke patients and rats. Research later showed that HA derived from probiotic *L.Reu* could suppress TNF *via* modulation of PKA and ERK signaling, and the protective effects of *L.Reu* against necrotizing enterocolitis were partially attributed to its ability to produce HA[22,25]. The neuroprotective effect of HA on OGD/R-PC12 cells was studied, and the results showed that exogenous HIS (0.1−1.0 μmol/L) could dose-dependently reduce the apoptosis rate, improve viability, and regulate pro-inflammatory factors of OGD/R-PC12 cells. Therefore, the HIS produced in *L.Reu* exerted therapeutic effects on obsolete IS through biotransformation into HA.

Based on the relative studies in recent years, three potential pathways might be involved in the neuroprotective effect of HIS along the gut−brain axis: the HPA axis, the vagal signaling, and the peripheral pathway. As to the signaling pathway from brain to gut microbiota, the HPA axis is regarded as the primary neuroendocrine system that regulates various physiological processes in response to psychological and physical stressors[48]. According to the literature reports, acute cerebral ischemia triggered by a transient ischemic attack sets off an intricate cascade of events within the central nervous system and the HPA axis, potentially leading to neuronal and cellular harm[49]. It was consistent with our findings that during the acute phase of IS, the metabolome in mice and patients was changed dramatically by acute ischemic attack, characterized by a notable rise in HIS levels observed in both mouse brain tissue and systemic circulation of mice and patients. However, as the disease

progressed, the HIS and HA levels decreased significantly in mice and patients with obsolete IS, which could be reversed by the colonization of *L. Reus*. Therefore, we herein focus on the interaction along gut−brain axis in the obsolete IS phase in terms of vagal signaling and the peripheral pathway. Intestinal microorganisms promote host nutrition by mediating the production of various metabolites, some of which may be transmitted into the brain through the vagus nerve pathway. Both in health and disease (including stroke), the gut microbiota could transmit signals from the gut microbiota to the brain through the vagus nerve, and vice versa, thereby affecting the CNS[22]. Increasing evidence suggested that alterations in the composition of gut microbiota were closely related to changes in host physiology, which could be eliminated through subphrenic vagotomy[50,51]. Therefore, the vagus nerve sensory pathway plays an indispensable role in connecting the brain−gut axis by transmitting microbial metabolites to the brain. Herein, to explore how the HIS produced by *L.Reu* plays a therapeutic role in obsolete IS, we severed the vagus nerve of I/R rats, established an I/R-V composite animal model, and compared the efficacy of HIS on I/R and I/R-V model rats. Our results demonstrated that vagotomy did not have a significant effect on the efficacy of HIS. We also found that vagotomy did not affect the up-regulation of HIS and HA exposure in the brain of I/R rats after PNS administration. According to previous reports, the synthesis of HA in the brain mainly depends on the concentration of HIS[52]. Therefore, PNS could promote the synthesis of HIS in the gut by up-regulating *L.Reu*, thereby increasing the HIS exposure in the brain through peripheral pathways. HIS, in turn, produced an active metabolite HA through decarboxylation, thereby exerting an indirect therapeutic effect on obsolete IS.

5. Conclusions

Our research findings proved for the first time that PNS could exert a significant therapeutic effect on IS, and this therapeutic effect was microbiota-dependent. Additionally, IS resulted in a significant down-regulation of *Lactobacilli* in rats, and PNS administration for consecutive 14 days dramatically enhanced the population of *Lactobacilli* in I/R rats, especially for *L.Reu*. Metabolomic analysis showed a significant reduction in serum HIS in clinical obsolete IS patients and rehabilitation period I/R rats. Meanwhile, the *L.Reu* colonization in I/R rats exhibited significant neuroprotective activity and greatly increased HIS in the systemic circulation. More importantly, exogenous HIS innovatively demonstrated indirect neuroprotective effects through metabolizing to HA. Notably, vagus nerve severance in I/R rats was performed to investigate HIS's neuroprotective mechanism. The results firstly revealed that PNS could promote HIS synthesis in gut by enhancing *L.Reu* proportion, thereby increasing intracerebral HA through peripheral pathway. Consequently, our data provided novel insights into HIS metabolism mediated by *L.Reu* in the pathogenesis and treatment of IS.

Acknowledgments

This study was supported by the National Natural Science Foundation of China (82274194), the Jiangsu Natural Science Funds (BK20211224, China), the Natural Science Foundation of Hebei Province (H2020208025, H2021208006, H2021302001, C2021418001, China), and the CAMS Innovation Fund for Medical Sciences (2021-I2M-5-011, China).

Author contributions

Kangrui Hu: Writing − original draft, Methodology, Formal analysis, Data curation. Zhihao Zhou: Formal analysis, Data curation. Haofeng Li: Formal analysis, Data curation. Jijun Xiao: Investigation, Funding acquisition. Yun Shen: Project administration, Methodology. Ke Ding: Software, Resources. Tingting Zhang: Visualization, Validation. Guangji Wang: Writing − review & editing, Supervision, Conceptualization. Haiping Hao: Writing − review & editing, Supervision, Conceptualization. Yan Liang: Writing − review & editing, Writing − original draft, Supervision, Conceptualization.

Conflicts of interest

The authors report there are no competing interests to declare.

Appendix A. Supporting information

Supporting information to this article can be found online at https://doi.org/10.1016/j.apsb.2024.10.003.

References

1. Wu S, Wu B, Liu M, Chen Z, Wang W, Anderson CS, et al. Stroke in China: advances and challenges in epidemiology, prevention, and management. *Lancet Neurol* 2019;**18**:394−405.
2. Warner JJ, Harrington RA, Sacco RL, Elkind MSV. Guidelines for the early management of patients with acute ischemic stroke: 2019 update to the 2018 guidelines for the early management of acute ischemic stroke. *Stroke* 2019;**50**:3331−2.
3. Qiu YM, Zhang CL, Chen AQ, Wang HL, Zhou YF, Li YN, et al. Immune cells in the BBB disruption after acute ischemic stroke: targets for immune therapy?. *Front Immunol* 2021;**12**:678744.
4. Qin J, Li R, Raes J, Arumugam M, Burgdorf KS, Manichanh C, et al. A human gut microbial gene catalogue established by metagenomic sequencing. *Nature* 2010;**464**:59−65.
5. Nakai H, Murosaki S, Yamamoto Y, Furutani M, Matsuoka R, Hirose Y. Safety and efficacy of using heat-killed *Lactobacillus plantarum* L-137: high-dose and long-term use effects on immune-related safety and intestinal bacterial flora. *J Immunotoxicol* 2021; **18**:127−35.
6. Cao Y, Li R, Bai L. Vagal sensory pathway for the gut−brain communication. *Semin Cel Dev Biol* 2024;**156**:228−43.
7. Weiser MJ, Handa RJ. Estrogen impairs glucocorticoid dependent negative feedback on the hypothalamic−pituitary−adrenal axis *via* estrogen receptor alpha within the hypothalamus. *Neuroscience* 2009; **159**:883−95.
8. Benakis C, Liesz A. The gut−brain axis in ischemic stroke: its relevance in pathology and as a therapeutic target. *Neurol Res Pract* 2022; **4**:57.
9. Hoofnagle AN, Resing KA, Ahn NG. Protein analysis by hydrogen exchange mass spectrometry. *Annu Rev Biophys Biomol Struct* 2003; **32**:1−25.
10. Singh V, Roth S, Llovera G, Sadler R, Garzetti D, Stecher B, et al. Microbiota dysbiosis controls the neuroinflammatory response after stroke. *J Neurosci* 2016;**36**:7428−40.
11. Karlsson FH, Fåk F, Nookaew I, Tremaroli V, Fagerberg B, Petranovic D, et al. Symptomatic atherosclerosis is associated with an altered gut metagenome. *Nat Commun* 2012;**3**:1245.
12. Zeng X, Gao X, Peng Y, Wu Q, Zhu J, Tan C, et al. Higher risk of stroke is correlated with increased opportunistic pathogen load and reduced levels of butyrate-producing bacteria in the gut. *Front Cel Infect Microbiol* 2019;**9**:4.

13. Zhang K, Chen L, Yang J, Liu J, Li J, Liu Y, et al. Gut microbiota-derived short-chain fatty acids ameliorate methamphetamine-induced depression- and anxiety-like behaviors in a Sigmar-1 receptor-dependent manner. *Acta Pharm Sin B* 2023;**13**:4801−22.
14. Erny D, De Angelis ALH, Jaitin D, Wieghofer P, Staszewski O, David E, et al. Host microbiota constantly control maturation and function of microglia in the CNS. *Nat Neurosci* 2015;**18**:965−77.
15. Sadler R, Cramer JV, Heindl S, Kostidis S, Betz D, Zuurbier KR, et al. Short-chain fatty acids improve poststroke recovery *via* immunological mechanisms. *J Neurosci* 2020;**40**:1162−73.
16. Agus A, Planchais J, Sokol H. Gut microbiota regulation of tryptophan metabolism in health and disease. *Cell Host Microbe* 2018;**23**:716−24.
17. Montgomery TL, Künstner A, Kennedy JJ, Fang Q, Asarian L, Culp-Hill R, et al. Interactions between host genetics and gut microbiota determine susceptibility to CNS autoimmunity. *Proc Natl Acad Sci U S A* 2020;**117**:27516−27.
18. Liao J, Cao Y, Zhao J, Yu B, Wang Y, Li W, et al. Aqueous extract of *Polygala japonica* Houtt. ameliorated nonalcoholic steatohepatitis in mice through restoring the gut microbiota disorders and affecting the metabolites in feces and liver. *Phytomedicine* 2023;**118**:154937.
19. Dai H, Kaneko K, Kato H, Fujii S, Jing Y, Xu A, et al. Selective cognitive dysfunction in mice lacking histamine H1 and H2 receptors. *Neurosci Res* 2007;**57**:306−13.
20. Zhu T, Wang L, Feng Y, Sun G, Sun X. Classical active ingredients and extracts of Chinese herbal medicines: pharmacokinetics, pharmacodynamics, and molecular mechanisms for ischemic stroke. *Oxid Med Cel Longev* 2021;**2021**:8868941.
21. Ahsan A, Liu M, Zheng Y, Yan W, Pan L, Li Y, et al. Natural compounds modulate the autophagy with potential implication of stroke. *Acta Pharm Sin B* 2021;**11**:1708−20.
22. Spielman LJ, Gibson DL, Klegeris A. Unhealthy gut, unhealthy brain: the role of the intestinal microbiota in neurodegenerative diseases. *Neurochem Int* 2018;**120**:149−63.
23. Xu ZY, Xu Y, Xie X fang, Tian Y, Sui J hui, Sun Y, et al. Anti-platelet aggregation of *Panax notoginseng* triol saponins by regulating GP1BA for ischemic stroke therapy. *Chin Med* 2021;**16**:12.
24. Li H, Xiao J, Li X, Chen H, Kang D, Shao Y, et al. Low cerebral exposure cannot hinder the neuroprotective effects of panax notoginsenosides. *Drug Metab Dispos* 2018;**46**:53−65.
25. Shelby RD, Mar P, Janzow GE, Mashburn-Warren L, Tengberg N, Navarro JB, et al. Antibacterial and anti-inflammatory effects of *Lactobacillus reuteri* in its biofilm state contribute to its beneficial effects in a rat model of experimental necrotizing enterocolitis. *J Pediatr Surg* 2022;**57**:1382−90.
26. Fu X, Chen K, Li Z, Fan H, Xu B, Liu M, et al. Pharmacokinetics and oral bioavailability of *Panax notoginseng* saponins administered to rats using a validated UPLC−MS/MS Method. *J Agric Food Chem* 2022;**71**:469−79.
27. Nakamura T, Naganuma F, Kudomi U, Roh S, Yanai K, Yoshikawa T. Oral histidine intake improves working memory through the activation of histaminergic nervous system in mice. *Biochem Biophys Res Commun* 2022;**609**:141−8.
28. Abrahams SL, Younathan ES. Modulation of the kinetic properties of phosphofructokinase by ammonium ions. *J Biol Chem* 1971;**246**:2464−7.
29. Jiang Z, Li L, Liu L, Ding B, Yang Y, He F, et al. Ischemic stroke and dysbiosis of gut microbiota: changes to LPS levels and effects on functional outcomes. *Altern Ther Health Med* 2023;**29**:284−92.
30. Abbafati C, Abbas KM, Abbasi M, Abbasifard M, Abbasi-Kangevari M, Abbastabar H, et al. Global burden of 369 diseases and injuries in 204 countries and territories, 1990−2019: a systematic analysis for the Global Burden of Disease Study 2019. *Lancet* 2020;**396**:1204−22.
31. Gottlieb M, Meissner H, Kalina M. What is the efficacy and safety of intravenous thrombolysis and thrombectomy among patients with a wake-up stroke?. *Ann Emerg Med* 2022;**80**:165−7.
32. Xie W, Meng X, Zhai Y, Zhou P, Ye T, Wang Z, et al. *Panax notoginseng* saponins: a review of its mechanisms of antidepressant or anxiolytic effects and network analysis on phytochemistry and pharmacology. *Molecules* 2018;**23**:940.
33. Liu Z, Zhang Q, Ding L, Li C, Yin Z, Yan G, et al. Preparation procedure and pharmacokinetic study of water-in-oil nanoemulsion of *Panax notoginseng* saponins for improving the oral bioavailability. *Curr Drug Deliv* 2016;**13**:600−10.
34. Guo Q, Li P, Wang Z, Cheng Y, Wu H, Yang B, et al. Brain distribution pharmacokinetics and integrated pharmacokinetics of *Panax* notoginsenoside R1, ginsenosides Rg1, Rb1, Re and Rd in rats after intranasal administration of *Panax Notoginseng* saponins assessed by UPLC/MS/MS. *J Chromatogr, B: Anal Technol Biomed Life Sci* 2014;**969**:264−71.
35. Arya A, Hu B. Brain−gut axis after stroke. *Brain Circ* 2018;**4**:165.
36. Xiao J, Chen H, Fu H, Ye W, Rao T, Shao Y, et al. Development of a novel sectional multiple filtering scheme for rapid screening and classifying metabolites of ziyuglycoside II in rat liver and excreta specimen based on high-resolution mass spectrometry. *J Pharm Biomed Anal* 2016;**129**:310−9.
37. Chervinets VM, Chervinets YV, Chichanovskaja LV, Ganzja DV, Grigoryants EO, Belyaev VS, et al. The spectrum of gas signaling molecules of intestinal lactobacilli in patients with ischemic stroke. *Klin Lab Diagnostika* 2022;**67**:163−9.
38. Rahman Z, Bhale NA, Dikundwar AG, Dandekar MP. Multistrain probiotics with fructooligosaccharides improve middle cerebral artery occlusion−driven neurological deficits by revamping microbiota−gut−brain axis. *Probiotics Antimicrob Proteins* 2023;**16**:1251−69.
39. Montgomery TL, Eckstrom K, Lile KH, Caldwell S, Heney ER, Lahue KG, et al. *Lactobacillus reuteri* tryptophan metabolism promotes host susceptibility to CNS autoimmunity. *Microbiome* 2022;**10**:198.
40. Krautkramer KA, Fan J, Bäckhed F. Gut microbial metabolites as multi-kingdom intermediates. *Nat Rev Microbiol* 2021;**19**:77−94.
41. Zheng X, Cai X, Hao H. Emerging targetome and signalome landscape of gut microbial metabolites. *Cell Metab* 2022;**34**:35−58.
42. Guido G, Crivellaro E, De Fortunato G, Melloni L. Sex and age dimorphism of the gut−brain axis in ischemic stroke: a systematic review of preliminary studies. *Brain Res* 2022;**1784**:147888.
43. Blasco MP, Chauhan A, Honarpisheh P, Ahnstedt H, D'Aigle J, Ganesan A, et al. Age-dependent involvement of gut mast cells and histamine in post-stroke inflammation. *J Neuroinflammation* 2020;**17**:160.
44. Brosnan ME, Brosnan JT. Histidine metabolism and function. *J Nutr* 2020;**150**:2570S−5S.
45. Niu YC, Feng RN, Hou Y, Li K, Kang Z, Wang J, et al. Histidine and arginine are associated with inflammation and oxidative stress in obese women. *Br J Nutr* 2012;**108**:57−61.
46. Yoshikawa T, Nakamura T, Shibakusa T, Sugita M, Naganuma F, Iida T, et al. Insufficient intake of L-histidine reduces brain histamine and causes anxiety-like behaviors in male mice. *J Nutr* 2014;**144**:1637−41.
47. Greaves MW, Sabroe RA. Histamine: the quintessential mediator. *J Dermatol* 1996;**23**:735−40.
48. Skowrońska M, Albrecht J. Oxidative and nitrosative stress in ammonia neurotoxicity. *Neurochem Int* 2013;**62**:731−7.
49. Radak D, Resanovic I, Isenovic ER. Changes in hypothalamus-pituitary-adrenal axis following transient ischemic attack. *Angiology* 2014;**65**:723−32.
50. Bravo JA, Forsythe P, Chew MV, Escaravage E, Savignac HM, Dinan TG, et al. Ingestion of *Lactobacillus* strain regulates emotional behavior and central GABA receptor expression in a mouse *via* the vagus nerve. *Proc Natl Acad Sci U S A* 2011;**108**:16050−5.
51. Sgritta M, Dooling SW, Buffington SA, Momin EN, Francis MB, Britton RA, et al. Mechanisms underlying microbial-mediated changes in social behavior in mouse models of autism spectrum disorder. *Neuron* 2019;**101**:246−259.e6.
52. Prell GD, Hough LB, Khandelwal J, Green JP. Lack of a precursor-product relationship between histamine and its metabolites in brain after histidine loading. *J Neurochem* 1996;**67**:1938−44.